Hindawi
International Transactions on Electrical Energy Systems
Volume 2022, Article ID 5339630, 31 pages
https://doi.org/10.1155/2022/5339630

*Research Article*

# Design and Analysis of FOPID-Based Damping Controllers Using a Modified Grey Wolf Optimization Algorithm

**Manoj Kumar Kar**,[1] **Sanjay Kumar**,[1] **Arun Kumar Singh**,[1] **Sibarama Panigrahi**,[2] **and Murthy Cherukuri**[3]

[1]*Electrical Engineering Department, National Institute of Technology, Jamshedpur, India*
[2]*Department of Computer Science Engineering & Application, SUIIT, Burla, India*
[3]*Department of Electrical & Electronics Engineering, NIST Institute of Science and Technology, Berhampur, India*

Correspondence should be addressed to Murthy Cherukuri; chmurthy@nist.edu

Received 15 June 2022; Revised 27 September 2022; Accepted 5 October 2022; Published 17 October 2022

Academic Editor: Pawan Sharma



This study proposes a novel modified grey-wolf optimization algorithm (MGWOA) to enhance power system stability. The power system stabilizer and static synchronous series compensator (SSSC) are used as damping controllers. Additionally, fractional-order PID (FOPID) controller is used to handle the system nonlinearities and thus achieve better performance. The control parameters are tuned using the proposed MGWOA method which has been verified on unimodal and multimodal functions. Single-machine infinite bus (SMIB) and multimachine power system (MMPS) are taken as case studies to analyze the efficacy of the proposed controller. Minimization of rotor speed deviation is considered an objective function. The results obtained from the MGWOA-tuned FOPID-based damping controllers are compared with those obtained using recently developed efficient and competitive heuristic algorithms. It was observed that the MGWOA method is well-suited for damping low-frequency oscillations. Furthermore, statistical analysis is performed on the obtained results to justify the superiority of the MGWOA method. The simulation results suggest that the MGWOA exhibits superior performance characteristics when applied to a real power system.

## 1. Introduction

*1.1. Background.* Power system stability is a major concern for the last few decades. Low-frequency oscillations are caused by fluctuations in the rotor angle and can cause power system instability which can lead to blackouts. There are several strategies discussed in [1] to provide adequate damping.

Power system stabilizer (PSS) generally produces an additional control signal which is provided to the excitation system for mitigating both the local and interarea mode oscillations. However, to achieve improved performance, tuning of the controller parameters is the main challenge for researchers in recent times. The parameters of PSS were tuned using the integral-square-error and phase compensation technique to analyze the dynamic performance of the system in [2]. Though the optimum PSS performs better in light and nominal loading, still performance has to be improved in heavy loading conditions. The interarea mode oscillations are efficiently damped by using an adaptive fuzzy PSS in [3]. The PSS parameters are optimized using the BAT search algorithm in [4], and the results were compared with GA-tuned PSS under different operating conditions. Similarly, GA is used in [5] to tune PSS parameters, but in this case, it is applied to MMPS. However, both GA and neural network methods were used to suppress small signal oscillations [6].

Later, FACTS controllers have been introduced to improve stability, damp rotor oscillations, control power flow, etc. [7]. The SSSC's performance is compared to that of a TCSC in [8] depending on a series capacitor. Wang [9] introduced SSSC effectively to SMIB and MMPS for

dampening the system oscillations. Using a modified GA method, the parameters of damping controllers are managed in [10].

PSS and FACTS controllers were designed for a sixteen-machine system, and the positioning of controllers was determined using the participation factor and residue technique [11]. Real-coded GA was used to tune the SSSC controller parameters in [12] which are applied to both SMIB and MMPS. Both local and remote signals are compared considering time delays. Using DE, a time delay-based SSSC controller design was suggested, and it was discovered that the remote signal performs better than the local signal when the delay is taken into account [13]. To improve the transient stability, a GA-based method [14] and DE method [15] are provided for developing the SSSC controller. The effect of SSSC on a SMIB considering subsynchronous resonance under heavy loading conditions was investigated in [16], and it was determined that SSSC maintained the operating point stability. An SSSC controller is developed, as well as a tuning mechanism that makes use of a multimodal decomposition was proposed to mitigate strong resonance in [17]. The SOA approach is offered as a means of coordinating the PSS and SSSC controllers to dampen oscillations and increase stability [18]. The multimachine PSS was designed in [19] using improved WOA and time-domain analysis was used to justify the efficacy of the proposed technique. To improve the power system stability, a novel modified SCA optimal coordinated design of damping controllers, i.e., PSS and SSSC controllers, are proposed [20].

Additionally, some other controllers are being used by the researchers along with FACTS controllers for improving the system's performance. PI and fuzzy logic controllers along with different FACTS controllers were suggested in [21] for mitigating power quality issues. To dampen low-frequency oscillations, a new coordinated controller, fuzzy-PID with the lead-lag term, and TCSC with POD structure were developed [22]. By minimizing an eigenvalue-based objective function using improved WOA, the PSS is constructed in [23] for the lower-order model of the modified SMIB system. A cascaded PID controller was proposed in [24] using a marine predator algorithm to improve rotor angle stability. To deal with nonlinearities efficiently, a novel fractional order PID (FOPID) controller was introduced by Podlubny [25]. The DE algorithm is modified to efficiently design the settings of the FOPID controllers in [26]. The parameters of the fractional-order PI controller were tuned to justify the robustness of the proposed controller for loop gain variations [27]. In [28], FOPID-PSS controller is proposed and its efficacy was compared with PID-PSS and PSS controller using the BAT algorithm. Later, different variants of the FOPID controller were used using the SCA method and the robustness of SCA-tuned FOPIDFF was justified in [29]. To improve power system stability, MWOA optimized fractional-order MISO-type SSSC controller was proposed by Sahu et al. in [30]. The deterministic and probabilistic approaches to optimizing PSS parameters to increase low-frequency oscillatory stability were proposed in [31]. Improved atomic search algorithm-based PSS was used considerably to improve the transient stability of the SMIB system and hence the damping properties of electromechanical modes, confirming the algorithm's exceptional performance [32]. In MMPS, dampening of local and interarea oscillation was accomplished [33]. However, as additional calculation and parametric information are required, this method becomes more complicated. The PSS parameters in MMPS are tuned using the PSO method in [34]. Furthermore, the damping factor and eigenvalue analysis are used to achieve the stability criteria. To optimize the PSS parameters, MMPS was subjected to a hybrid-modified GWO technique [35]. In addition, the proposed method was subjected to a statistical analysis test to demonstrate its superiority over alternative approaches. The PSS parameters were set utilizing a hybrid MGWO-SCA method to provide improved system performance characteristics in [36] by increasing the damping nature of the system states during abnormal operating conditions. To improve power system stability, Sahu et al. [37] proposed an adaptive fuzzy lead-lag controller structure for power system stabilizer and SSSC-based damping controllers. A modified grasshopper optimization algorithm was used to tune the parameters of the proposed controller. Also, some researchers incorporated renewable sources with FACTS controllers to improve small signal stability and to damp low frequency oscillations. A SSSC and governor were proposed for the critical condition of a power system for small signal stability enhancement, taking into account sudden and random variations in photovoltaic and wind sources, as well as different operating conditions of hydrogeneration and changes in reference voltage [38]. A detailed eigenvalue analysis using time-domain simulations was carried out to investigate the damped oscillatory response of variable and random solar penetration with a power system, as well as the interaction of solar power with variable synchronous power generation [39].

Although using PSS, FACTS, or coordination of both the controllers improves the system stability by damping low-frequency oscillations, some researchers considered additional controllers such as PI and fuzzy logic controller, fuzzy-PID, and cascaded PID with better performance. In this study, the authors proposed a FOPID controller whose parameters are tuned by the modified GWO technique. Additionally, a statistical analysis has been performed on fitness values to justify the effectiveness of the proposed approach.

*1.2. Novelty and Paper Layout.* The novelty and layout of this study are given as below:

(i) A modified grey wolf optimization algorithm (MGWOA) is proposed to design a FOPID-PSS controller to enhance the power system stability.

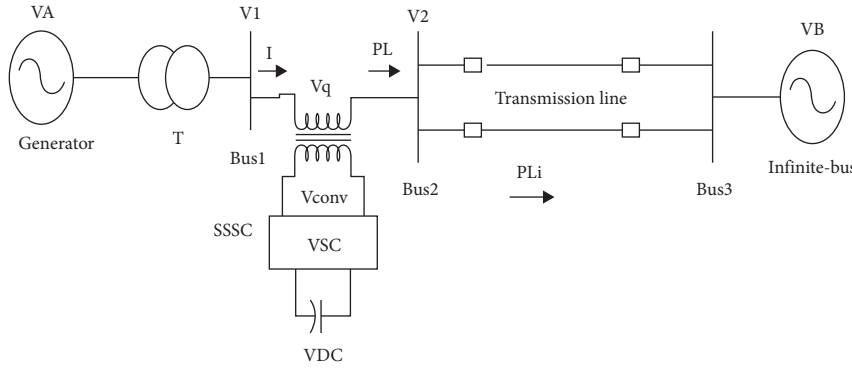


Figure 1: SSSC incorporated single-machine infinite bus system.

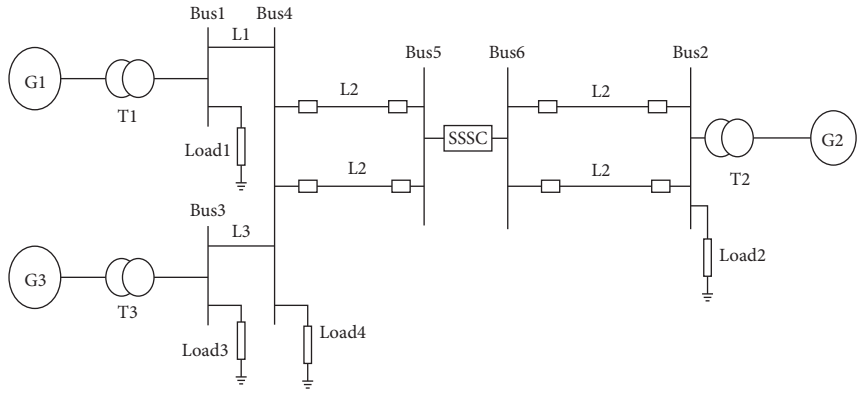


Figure 2: SSSC incorporated multimachine power system.

(ii) The MGWOA approach is used to optimize the controller parameters of the SMIB and MMPS considering different loading conditions.

(iii) The superiority of the MGWOA method is tested using unimodal and multimodal functions.

(iv) As comparison approaches, six potential optimization algorithms such as GWO, SSA, MSCA, SCA, ALO, and DE are used.

(v) Because metaheuristic algorithms are inherently stochastic, statistical analysis on the obtained results is performed. Furthermore, the Wilcoxon signed-rank test (WSRT) is used for the first time after employing the FOPID controller to draw conclusions.

The structure of the study is as follows. The case studies and various types of controllers are described in Section 2. The problem formulation is stated in Section 3. Section 4 explains the proposed MGWOA approach in detail. The performance of the MGWOA method using benchmark functions and statistical analysis is presented in Section 5. In Sections 6 and 7, the MGWOA approach is implemented on the SMIB system and MMPS, respectively, and finally, the findings are concluded in Section 8.

## 2. Case Studies

*2.1. Case Study 1.* The first system considered for analysis is a single machine infinite bus. It consists of a generator (2100 MVA, 13.8 kV, 60 Hz), a 3-phase transformer (13.8 kV/500 kV) which is connected to an infinite bus (500 kV, 15000 MVA) via two 500 kV transmission lines of length 200 km and 300 km each, as shown in Figure 1. SSSC (100 MVA) is incorporated in series with the transmission lines. The terminal voltage is denoted as $V_A$ and the infinite bus voltage is denoted as $V_B$.

*2.2. Case Study 2.* The second system is the multimachine power system (MMPS), which consists of 6 buses, 4 number of loads (250 MW, 50 MW, 250 MW), and 3 generators (with ratings 2100 MVA, 4200 MVA, and 2100 MVA) that forms two subsections, interlinked through a tie-line, as shown in Figure 2. The system data considered are shown in Appendix [20]. SSSC is connected between bus 5 and bus 6 for improving stability when any disturbance occurs. A three-phase fault is given between bus 2 and bus 6 for creating a disturbance. Each generator is having its PSS to stabilize the signals.

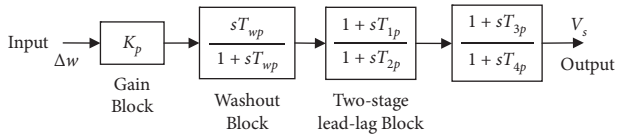


Figure 3: Block diagram of PSS.

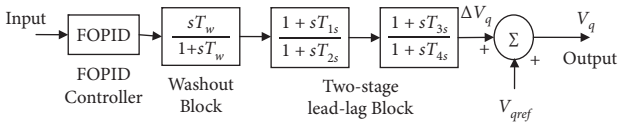


Figure 4: Structure of FOPID-based SSSC controller.

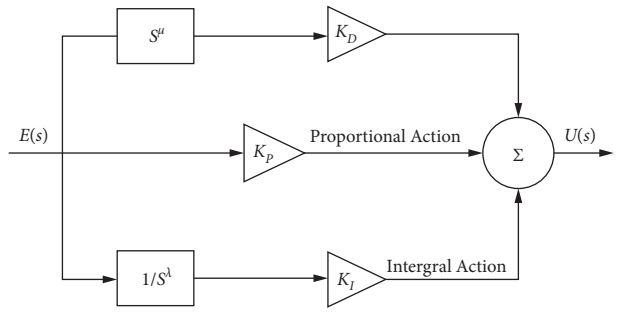


Figure 5: Structure of FOPID controller.

*2.3. Configuration of PSS and SSSC Damping Controller.* The PSS improves the system stability limit by regulating generator excitation to dampen synchronous machine rotor oscillations relative to one another. It generates an electrical torque component on the rotor that varies in phase with speed. The basic structure of a PSS is given in [1] and shown in Figure 3. The block diagram of PSS includes a gain block having to gain $K_{pss}$, a washout block that acts as a high pass filter, and a phase compensation block that provides required phase-lead characteristics for compensating any delay between the input and output signals. The amount of damping to be injected is determined by the stabilizer gain. To avoid steady-state error in the terminal voltage, a washout filter restricts it to acting only against oscillations in the input signal.

SSSC is a solid-state voltage sourced converter that produces a controlled alternating current voltage. The transmission line's impedance is virtually compensated, which is accomplished through the injection of the SSSC voltage into the transmission line. To modify the value of $V_q$, a VSC is coupled to the secondary side of a coupling transformer. The amplitude of $V_q$ can be changed to regulate the compensation level, and the system can be employed in capacitive or inductive mode. The structure of the SSSC controller is discussed in [12] and shown in Figure 4. FOPID controller handles the system nonlinearities and helps to improve the system performance. Rest blocks perform the same purpose as described in the case of PSS. The desired compensation value is obtained by changing the SSSC-injected voltage ($\Delta V_q$), which is added to the reference injected voltage ($V_{q\text{ref}}$).

*2.4. FOPID Controller.* An FOPID controller is based on fractional calculus and allows noninteger order integration and differentiation. This noninteger operator adds extra flexibility to engineering challenges. This controller with a fractional integrator and differentiator is commonly denoted as $PI^\lambda D^\mu$, where $\lambda$ is the integrator order and $\mu$ is the differentiator order. The structure of FOPID controller is given in Figure 5.

The transfer function of the FOPID controller is given by

$$\mathbf{G_{FOPID}(s)} = \mathbf{K_p} + \frac{\mathbf{K_I}}{\mathbf{S^\lambda}} + \mathbf{K_D S^\mu}, \tag{1}$$

where $\mathbf{K_p}$, $\mathbf{K_I}$, and $\mathbf{K_D}$ denote the proportional, integral, and differential gains, respectively.

## 3. Problem Formulations

It is worth noting that PSS- and SSSC-based damping controllers are intended to reduce power system oscillations following a large disturbance and, therefore, enhance power system stability. Deviations in power angle, rotor speed, and tie-line power reflect these oscillations. Minimization of any or all of the aforementioned deviations could be chosen as the objective. In this study, the objective is to minimize the speed deviation as much as possible. For a SMIB power system, the ITAE of the speed deviations is used as the objective function which is given as

$$\text{ITAE} = \int_0^{t_s} |\Delta\omega|.t\text{dt}, \tag{2}$$

where $\Delta\omega$ represents speed deviation and $t_s$ represents the simulation time.

The constraints are expressed as

MinimizeITAE

Subject to

$$\begin{aligned} K_{pss}^{\min} &\le K_{pss} \le K_{pss}^{\max} \\ T_{pm}^{\min} &\le T_{pm} \le T_{pm}^{\max}, \quad m = 1,2,3,4, \\ T_n^{\min} &\le T_n \le T_n^{\max}, \quad n = 1,2,3,4, \end{aligned} \tag{3}$$

where $K_{pss}^{\min}$ and $K_{pss}^{\max}$ are the minimum and maximum bounds for PSS gain, $T_{pm}^{\min}$ and $T_{pm}^{\max}$ represent the minimum and maximum bounds for the time constant of PSS, and $T_n^{\min}$ and $T_n^{\max}$ represent the minimum and maximum bounds for the time constant of SSSC.

The ITAE of the speed deviations w.r.t. local and interarea modes is taken as the objective function in MMPS and can be expressed as

$$\text{ITAE} = \int_0^{t_s} \left(\sum|\Delta\omega_L| + \sum|\Delta\omega_I|\right).t\text{dt}, \tag{4}$$

where $\Delta\omega_L$ and $\Delta\omega_I$ represent the local area and the interarea speed deviation, respectively.

The optimization problem can be stated as follows:

MinimizeITAE

Subject to

$$\begin{aligned} &K_{Px}^{\min} \le K_{Px} \le K_{Px}^{\max}, \quad x = 1, 2, 3, \\ &T_n^{\min} \le T_n \le T_n^{\max}, \quad n = 1, 2, 3, 4, \\ &T_{ab}^{\min} \le T_{ab} \le T_{ab}^{\max}, \quad a = 1, 2, 3 \text{ and } b = 1, 2, 3, 4, \end{aligned} \tag{5}$$

where $K_{Px}^{\min}$ and $K_{Px}^{\max}$ are the minimum and maximum bounds of the PSS gain, $T_n^{\min}$ and $T_n^{\max}$ represent the minimum and maximum bounds of time constant of SSSC, and $T_{ab}^{\min}$ and $T_{ab}^{\max}$ represent the minimum and maximum bounds of time constant for PSS. For the SMIB system, PSS, SSSC, and FOPID controllers are used. So, 14 parameters (4 gain, 8 time constant, and 2 fractional-order constant) are to be optimized. On the contrary, in the case of MMPS, 3 PSS, 1 SSSC, and 1 FOPID controller are used. Thus, 24 numbers of parameters (6 gain, 16 time constant, and 2 fractional-order constant) are to be optimized.

## 4. Proposed Approach

In 2014, Mirjalili et al. [40] proposed a novel metaheuristic algorithm inspired by leadership hierarchy and hunting behavior of grey wolves called grey wolf optimization (GWO). The grey wolf pack is divided into four tiers of leadership: alpha ($\alpha$), beta ($\beta$), delta ($\delta$), and omega ($\omega$). Alpha leads the group and dictates the group after taking decisions. Thus, alpha rules over all wolves and occupies the highest position in the grey wolf hierarchy. The second and third tiers of the hierarchy are beta and delta, who obey and assist the alpha in making decisions and dominating the rest of the wolves known as omega. Alpha is treated as the best optimal fitness solution, beta and delta correspond to the second best and the third-best solution,respectively, and the remaining solutions correspond to omega.

For the purposes of mathematical modelling of the hunting mechanism, it is considered that alpha, beta, and delta wolves have a solid understanding of prospective prey positions and that the omega wolves update their location based on the above three wolves. Accordingly, the mathematical formulas are mentioned as below:

$$\begin{aligned} \overrightarrow{D_\alpha} &= \left|\overrightarrow{C_1}.\overrightarrow{X_\alpha} - \overrightarrow{X_i}(t)\right|, \overrightarrow{D_\beta} = \left|\overrightarrow{C_2}.\overrightarrow{X_\beta} - \overrightarrow{X_i}(t)\right|, \overrightarrow{D_\delta} \\ &= \left|\overrightarrow{C_3}.\overrightarrow{X_\delta} - \overrightarrow{X_i}(t)\right|, \end{aligned} \tag{6}$$

$$\begin{aligned} \overrightarrow{X_1} &= \left|\overrightarrow{X_\alpha} - \overrightarrow{A_1}.\overrightarrow{D_\alpha}\right|, \overrightarrow{X_2} = \left|\overrightarrow{X_\beta} - \overrightarrow{A_2}.\overrightarrow{D_\beta}\right|, \overrightarrow{X_3} \\ &= \left|\overrightarrow{X_\delta} - \overrightarrow{A_3}.\overrightarrow{D_\delta}\right|, \end{aligned} \tag{7}$$

$$\overrightarrow{X_i}(t+1) = \frac{\overrightarrow{X_1} + \overrightarrow{X_2} + \overrightarrow{X_3}}{3}, \tag{8}$$

$$\overrightarrow{A} = 2\overrightarrow{a}.\overrightarrow{r_1} - \overrightarrow{a}, \tag{9}$$

$$\overrightarrow{C} = 2.\overrightarrow{r_2}, \tag{10}$$

$$\overrightarrow{a} = 2\left(1 - \frac{t}{T_{\max}}\right), \tag{11}$$

where $\overrightarrow{X_\alpha}$, $\overrightarrow{X_\beta}$, $\overrightarrow{X_\delta}$ and $\overrightarrow{D_\alpha}$, $\overrightarrow{D_\beta}$, $\overrightarrow{D_\delta}$ denote the position vectors and coefficient vectors of alpha, beta, and delta wolves, respectively. $\overrightarrow{X_i}(t)$ and $\overrightarrow{X_i}(t+1)$ represent the solution in current and next iterations, respectively. $\overrightarrow{A}$ and $\overrightarrow{C}$ represent the coefficient vectors. The components of $\overrightarrow{a}$ linearly decreased from 2 to 0 throughout iterations, while $\overrightarrow{r_1}$ and $\overrightarrow{r_2}$ are random vectors in the range [0, 1]. $T_{\max}$ is the maximum number of iterations.

GWO algorithm is simpler, more efficient, easier to use, and has a faster convergence rate when compared to other metaheuristic algorithms. However, this method is being trapped in local optima since the updated position is decided by the position of alpha, beta, and delta wolves causing an imbalance between exploration and exploitation. Therefore, in this study, a novel approach is proposed to further improve the performance of GWO and implemented to enhance stability.

In the case of MGWOA, a greater number of iterations are used for exploration and a smaller number of iterations are used for exploitation. A local search agent is used to identify the solution in case of exploitation. The expression of component $a$ (given in (11)), is modified as follows:

$$a = 2\left(1 - \frac{t^{1.5}}{T_{\max}^{1.5}}\right). \tag{12}$$

In the MGWO approach, the alpha is given 50% weightage, the beta is given 33.33% weightage, and the delta is given 16.66% weightage. The expression for the updated position using MGWO is given by

$$\overrightarrow{X_i}(t+1) = \frac{3\overrightarrow{X_1} + 2\overrightarrow{X_2} + \overrightarrow{X_3}}{6}. \tag{13}$$

The flowchart for the proposed MGWOA approach is presented in Figure 6. It has three stages: (i) initialization, (ii) iteration, and (iii) termination. In the first step, the different parameters such as maximum iteration ($T_{\max}$), number of search agents ($n$), parameter ($a$), the coefficient vectors $\overrightarrow{A}$ and $\overrightarrow{C}$ are initialized. For each search agent, three new search agents' positions get updated in the second step. The final (optimal) solution is given by the expression in equation (13). Finally, the best search agent from the final iteration is picked as the best solution to the problem.

## 5. Performance Analysis of MGWOA Approach

The performance of the MGWOA approach is evaluated using benchmark (unimodal and multimodal) functions. The results achieved by employing the proposed MGWOA approach are compared to certain well-known metaheuristic algorithms, notably, original GWO [35], MSCA [20], SCA

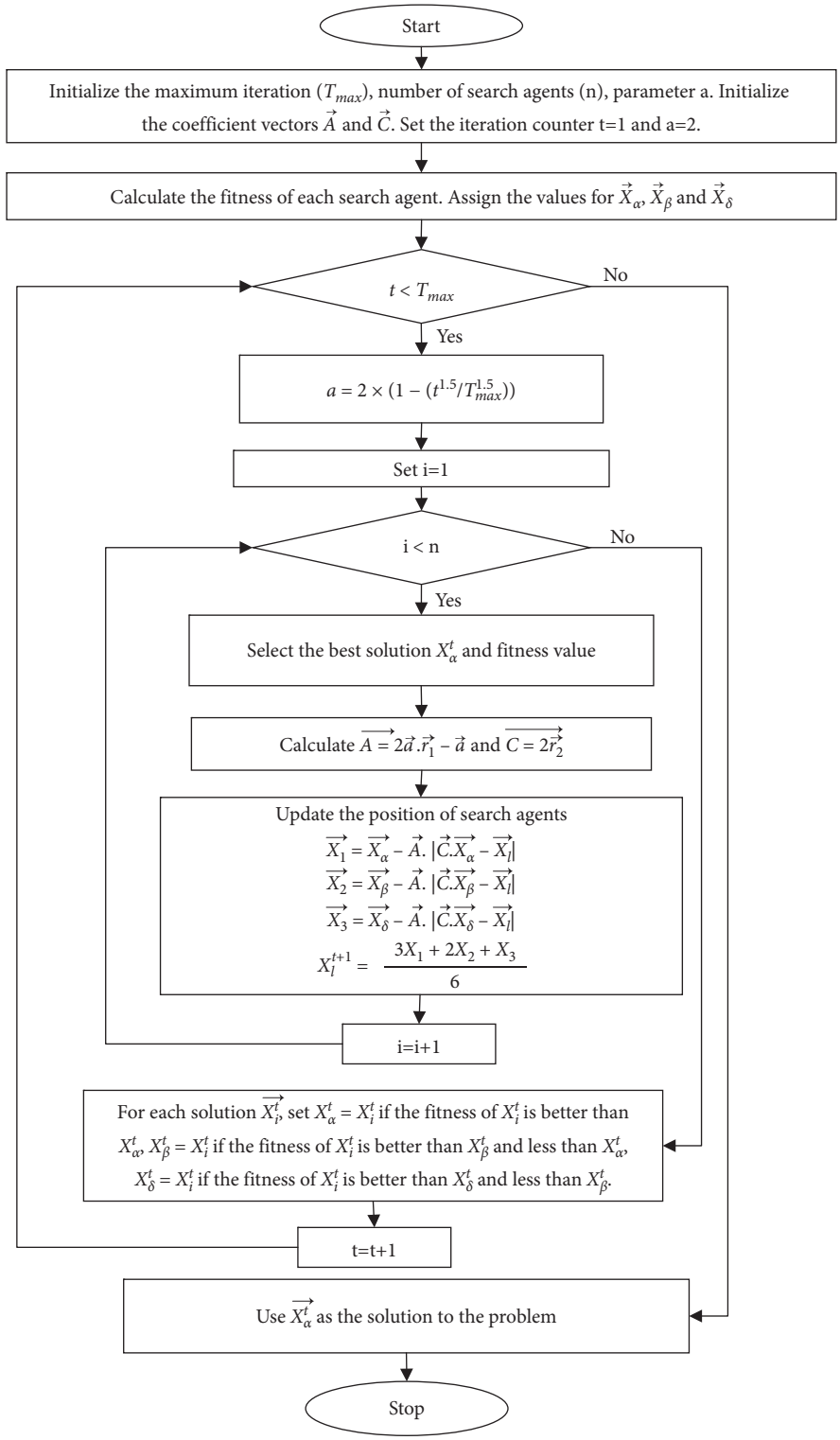


Figure 6: Flowchart of MGWOA approach.

[20], and DE [15]. All algorithms are run independently 15 times with 20 search agents and 500 iterations. The different unimodal and multimodal benchmark functions that are considered for performance evaluation are shown in Table 1.

Table 2 displays the mean and standard deviations of the benchmark functions. Table 2 shows that the MGWOA strategy outperforms all existing techniques in ten functions, i.e., $(F_1, F_2, F_3, F_4, F_5, F_7, F_9, F_{10}, F_{12}, F_{13})$; whereas SSA,

Table 1: Benchmark functions used for performance evaluation.

| Functions | Dimension | Range | $\mathbf{f_{min}}$ |
|---|---|---|---|
| $f_1(x) = \sum_{i=1}^{n} x_i^2$ | 30 | [−100, 100] | 0 |
| $f_2(x) = \sum_{i=1}^{n} \lvert x_i \rvert + \prod_{i=1}^{n} \lvert x_i \rvert$ | 30 | [−10, 10] | 0 |
| $f_3(x) = \sum_{i=1}^{n} (\sum_{j-1}^{i} x_j)^2$ | 30 | [−100, 100] | 0 |
| $f_4(x) = \max_i \{\lvert x_i \rvert,\ 1 \le i \le n\}$ | 30 | [−100, 100] | 0 |
| $f_5(x) = \sum_{i=1}^{n} [(x_{i+1} - x_i^2)^2 + (x_i - 1)^2]$ | 30 | [−30, 30] | 0 |
| $f_6(x) = n\sum_{i=1}^{n} ([x_i + 0.5]^2)$ | 30 | [−100, 100] | 0 |
| $f_7(x) = \sum_{i=1}^{n} i x_i^4 + \text{random}[0, 1]$ | 30 | [−100, 100] | 0 |
| $f_8(x) = \sum_{i=1}^{n} -x_i \sin(\sqrt{\lvert x_i \rvert})$ | 30 | [−500, 500] | 0 |
| $f_9(x) = \sum_{i=0}^{n} [x_i^2 - 10\cos(2\pi x_i) + 10]$ | 30 | [−5.12, 5.12] | 0 |
| $f_{10}(x) = -20\exp(-0.2\sqrt{(1/n)\sum_{i=1}^{n} x_i^2}) - \exp((1/n)\sum_{i=1}^{n} \cos(2\pi x_i)) + 20 + e$ | 30 | [−32, 32] | 0 |
| $f_{11}(x) = (1/4000)\sum_{i=1}^{n} x_i^2 - \prod_{i=1}^{n} \cos(x_i/\sqrt{i}) + 1$ | 30 | [−600, 600] | 0 |
| $f_{12}(x) = (\pi/n)\left\{10\sin(\pi y_1) + \sum_{i=1}^{n-1} (y_i - 1)^2 [1 + 10\sin^2(\pi y_{i+1})] + (y_{n-1})^2\right\} + \sum_{i=1}^{n} u(x_i, 10, 100, 4)$, $y_i = 1 + ((x_i + 1)/4)$, $u(x_i, a, k, m) = \begin{cases} k(x_i - a)^m & x_i > a \\ 0 & -a < x_i < a \\ k(-x_i - a)^m & x_i < -a \end{cases}$ | 30 | [−50, 50] | 0 |
| $f_{13}(x) = 0.1\left\{\sin^2(3\pi x_1) + \sum_{i=1}^{n} (x_i - 1)^2 [1 + \sin^2(3\pi x_i + 1)] + (x_n - 1)^2 [1 + \sin^2(2\pi x_n)]\right\} + \sum_{i=1}^{n} u(x_i, 5, 100, 4)$ | 30 | [−50, 50] | 0 |

DE, and GWO perform better than all other techniques in function $F_6$, $F_8$, and $F_{11}$, respectively. Because metaheuristic methods are stochastic in nature, therefore, statistical analysis on the generated data is required to draw definitive conclusions. As a result, WSRT [41, 42] is applied to the obtained results (at a 95% confidence level) to identify the inferiority (−), superiority (+), or equivalency ($\approx$) of a technique in contrast to the suggested MGWOA approach. Table 3 presents the WSRT results. Table 3 shows that the suggested MGWOA approach statistically outperforms the original GWO, SSA, MSCA, SCA, ALO, and DE methods in 1, 2, 3, 4, and 10 functions. The proposed MGWOA approach is statistically inferior to that of original GWO in functions 6 and 11, SSA and ALO in function 6, and DE in function 8, respectively. It provides statistically equivalence results with SSA and MSCA in function 5, DE in function 6, GWO and MSCA in function 7, GWO, SSA, MSCA, and ALO in function 8, MSCA in function 9: SSA, MSCA, SCA, ALO, and DE in function 11, and GWO and SSA both in functions 12 and 13. Furthermore, the semilog convergence graphs for 13 different functions are obtained and shown in Figures 7–19 to demonstrate the convergence properties of various techniques considered.

## 6. Analysis of SMIB System Using MGWOA Method

The design and simulation of FOPID-based damping controllers are carried out with the help of the Sim Power System toolkit. Figure 20 depicts the Simulink model for an SSSC-incorporated SMIB system. The SMIB model is then simulated with a disturbance, and the fitness value is then evaluated.

The responses of the different parameters under various loadings are described below.

### 6.1. Nominal Loading (NL) Condition

(i) The performance of the proposed controller is tested under nominal loading conditions ($P_e = 0.8$ pu) under disturbance.

(ii) A five-cycle, three-phase fault has been applied at $t = 1$ s. Once the fault has been resolved, the system is restored.

(iii) Figures 21–24 illustrate various responses such as speed deviation, power angle, tie line power $P$, and SSSC injected voltage $V_q$.

(iv) It is also obvious from the figures that the use of an MGWOA-based FOPID tuned damping controller improves the system's stability. Figure 25 shows the convergence curve of various algorithms under nominal loading cases.

### 6.2. Light Loading (LL) Condition

(i) A light loading ($P_e = 0.5$ pu) with a three-phase five-cycle fault at $t = 1$ s is assumed.

(ii) Figures 26–29 depict the efficacy of the suggested technique on various system responses to damp oscillation.

(iii) The superiority of the MGWOA approach over other methods considered in this study is justified by its better damping characteristics. Figure 30 shows the convergence curve of various algorithms under a light loading case.

### 6.3. Heavy Loading (HL) Condition

(i) To evaluate the performance of the suggested technique, heavy loading ($P_e = 0.95$pu) is used. Figures 31–34 depict the responses under heavy loading situations.

(ii) The figures clearly show that the proposed approach outperforms the other techniques considered in this study in terms of stability under various operating

Table 2: Comparison of results on unimodal and multimodal function using different optimization techniques (best values are presented in bold).

| Functions | MGWO<br>Mean ± Std. Dev | GWO<br>Mean ± Std. Dev | SSA<br>Mean ± Std. Dev | MSCA<br>Mean ± Std. Dev | SCA<br>Mean ± Std. Dev | ALO<br>Mean ± Std. Dev | DE<br>Mean ± Std. Dev |
|---|---|---|---|---|---|---|---|
| *F*1 | **8.48** $E-64$ ± **2.2** $E-63$ | $6.77E-47$ ± $1.5E-46$ | $1.12E-09$ ± $6.1E-10$ | $6.69E-28$ ± $2.09E-27$ | $2.48E-10$ ± $4.36E-10$ | $7.03E-08$ ± $1.16E-07$ | 0.013001 ± 0.036225 |
| *F*2 | **1.1** $E-37$ ± **1.38** $E-37$ | $4.36E-27$ ± $1.09E-26$ | 0.163709 ± 0.45983 | $1.07E-17$ ± $1.23E-17$ | $3.33E-09$ ± $5.1E-09$ | 1.015672 ± 1.390916 | $6.74E-05$ ± 0.000123 |
| *F*3 | **5.58** $E-29$ ± **1.126** $E-28$ | $1.75E-20$ ± $5.4E-20$ | 0.000316 ± 0.000592 | $9.66E-17$ ± $1.4E-16$ | 0.419762 ± 1.263159 | 12.50177 ± 22.18197 | 1.796805 ± 3.798125 |
| *F*4 | **1.22** $E-21$ ± **1.81** $E-21$ | $2.21E-15$ ± $2.69E-15$ | $3.7E-05$ ± $1.71E-05$ | $3.26201E-10$ ± $3.48E-10$ | 0.0003846 ± 0.000394 | 0.7401937 ± 1.507186 | 1.469459264 ± 2.716353 |
| *F*5 | **6.524987** ± **0.484725** | 7.0391 ± 0.296566 | 210.1478 ± 412.0016 | 6.954104 ± 0.705376 | 7.819536 ± 0.337342 | 484.3878 ± 620.3184 | 9103.372 ± 28438.58 |
| *F*6 | $1.39E-05$ ± $5.69E-06$ | $4.48E-06$ ± $1.16E-06$ | **1.13** $E-09$ ± **5.57** $E-10$ | 0.096951 ± 0.125587 | 0.649542 ± 0.199076 | $1.66E-07$ ± $2.69E-07$ | 0.015137 ± 0.036389 |
| *F*7 | **0.000668** ± **0.000579** | 0.001115 ± 0.000442 | 0.022117 ± 0.011898 | 0.001313 ± 0.00105 | 0.00311 ± 0.002841 | 0.042616 ± 0.01674 | 0.017685 ± 0.023621 |
| *F*8 | −2606.17 ± 454.2259 | −2552.27 ± 211 | −2715.65 ± 340.8558 | −2684.92 ± 277.6508 | −2045.58 ± 159.7924 | −2220.69 ± 340.1053 | **−3485.6** ± **270.7234** |
| *F*9 | **0** ± **0** | 2.255977 ± 2.839804 | 25.1724 ± 8.533826 | 0.205913 ± 0.651154 | 2.073695 ± 4.808659 | 25.57037 ± 8.753872 | 8.159463 ± 6.563448 |
| *F*10 | **5.15** $E-15$ ± **1.42** $E-15$ | $1.01E-14$ ± $3.62E-15$ | 1.078456 ± 0.809624 | 5.990833 ± 9.646164 | 0.355878 ± 1.104214 | 0.713261 ± 0.915327 | 1.530094 ± 1.359048 |
| *F*11 | 0.081252 ± 0.208098 | **0.031126** ± **0.025341** | 0.239618 ± 0.117724 | 0.059353 ± 0.043021 | 0.152399 ± 0.147993 | 0.219693 ± 0.090786 | 0.104326 ± 0.043356 |
| *F*12 | **0.003586** ± **0.007198** | 0.013586 ± 0.015119 | 0.701719 ± 1.146387 | 0.024783 ± 0.018141 | 0.119026 ± 0.051015 | 3.863013 ± 3.90695 | 0.829486 ± 1.106845 |
| *F*13 | **4.13** $E-05$ ± **2.4** $E-05$ | 0.030255 ± 0.046207 | 0.004303 ± 0.00745 | 0.05276 ± 0.071628 | 0.308826 ± 0.081058 | 0.011749 ± 0.008723 | 0.898463 ± 1.957858 |

Table 3: Wilcoxon signed-rank test results on unimodal and multimodal functions indicating the inferior (−), superior (+), or equivalent (≈) method in comparison to the proposed MGWOA method.

| | GWO | SSA | MSCA | SCA | ALO | DE |
|---|---|---|---|---|---|---|
| *F*1 | − | − | − | − | − | − |
| *F*2 | − | − | − | − | − | − |
| *F*3 | − | − | − | − | − | − |
| *F*4 | − | − | − | − | − | − |
| *F*5 | − | ≈ | ≈ | − | − | − |
| *F*6 | + | + | − | − | + | ≈ |
| *F*7 | ≈ | − | ≈ | − | − | − |
| *F*8 | ≈ | ≈ | ≈ | − | ≈ | + |
| *F*9 | − | − | ≈ | − | − | − |
| *F*10 | − | − | − | − | − | − |
| *F*11 | + | ≈ | ≈ | ≈ | ≈ | ≈ |
| *F*12 | ≈ | ≈ | − | − | − | − |
| *F*13 | ≈ | ≈ | − | − | − | − |

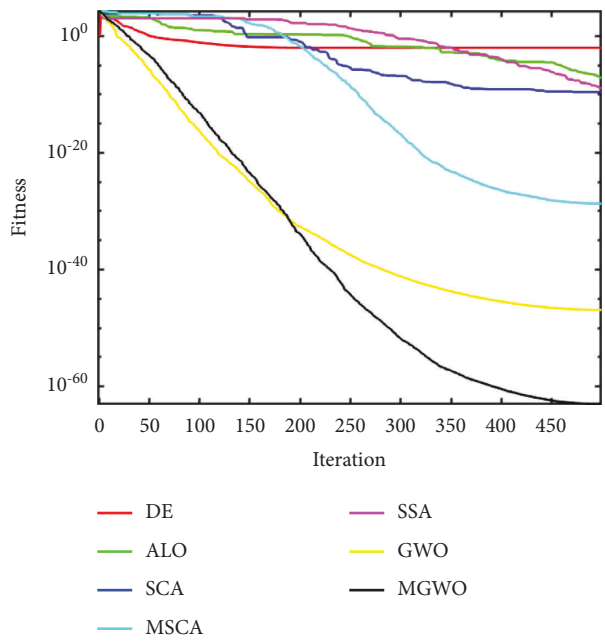


Figure 7: Convergence graph for *F*1 function.

situations. Figure 35 shows the convergence curve of various algorithms under heavy loading cases.

(iii) To assess MGWOA's effectiveness in finding the parameters of the SMIB system, fifteen independent simulations are run with MGWOA, GWO, SSA, MSCA, SCA, ALO, and DE.

(iv) The mean and standard deviations of fifteen independent runs for nominal loading, light loading, and heavy loading conditions are presented in Tables4–6, respectively.

(v) According to the tables, the proposed approach achieves the lowest mean among all the techniques taken for analysis. The optimized parameters of PSS, FOPID, and SSSC controllers obtained for SMIB system under nominal, light, and heavy loading conditions are presented in Tables 7–9, respectively, using the different methods.

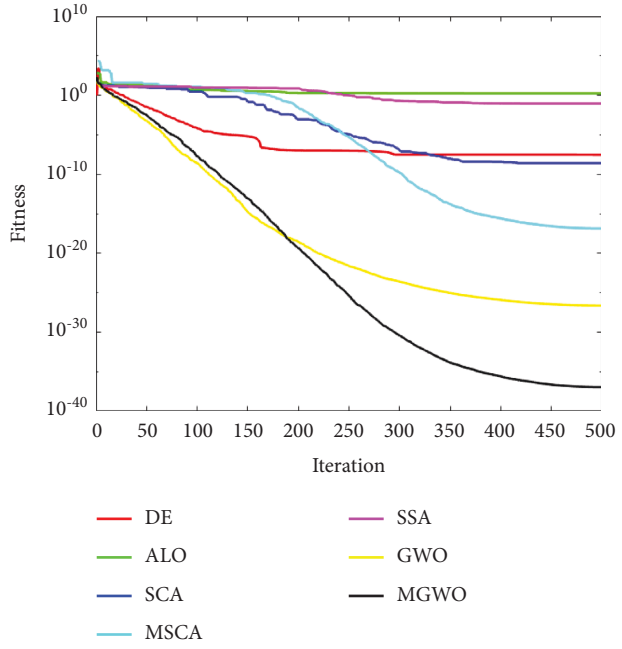


Figure 8: Convergence graph for $F2$ function.

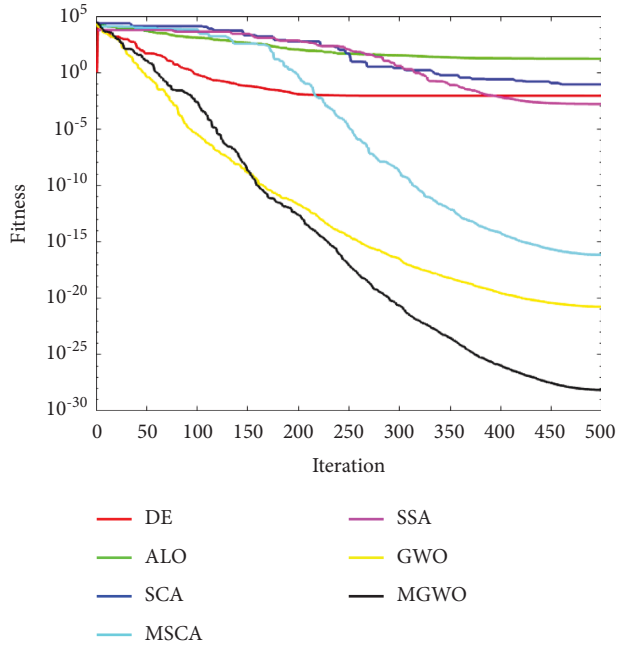


Figure 9: Convergence graph for $F3$ function.

## 7. Analysis of Multimachine Power System Using MGWOA

Figure 36 depicts the Simulink model for the MMPS network incorporating SSSC.

(i) The proposed approach is employed to optimize the parameters used in PSS, FOPID, and SSSC controller.

(ii) Following a disturbance, the two subsystems swing against one another, causing instability.

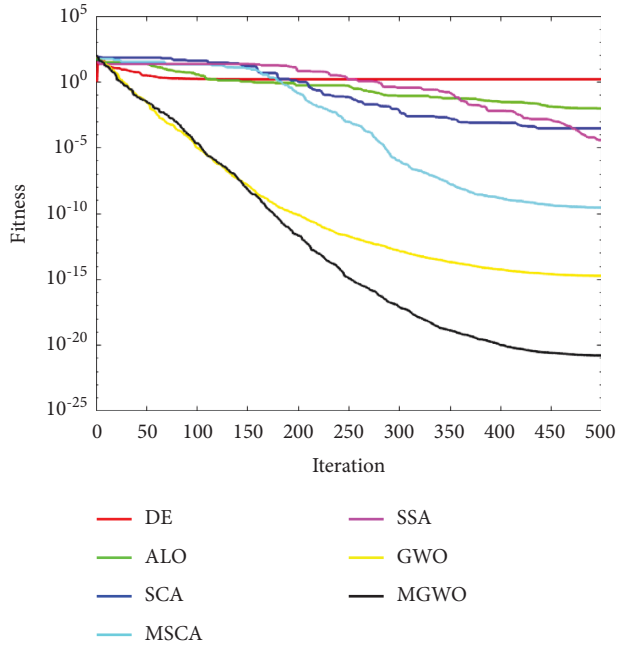


Figure 10: Convergence graph for $F4$ function.

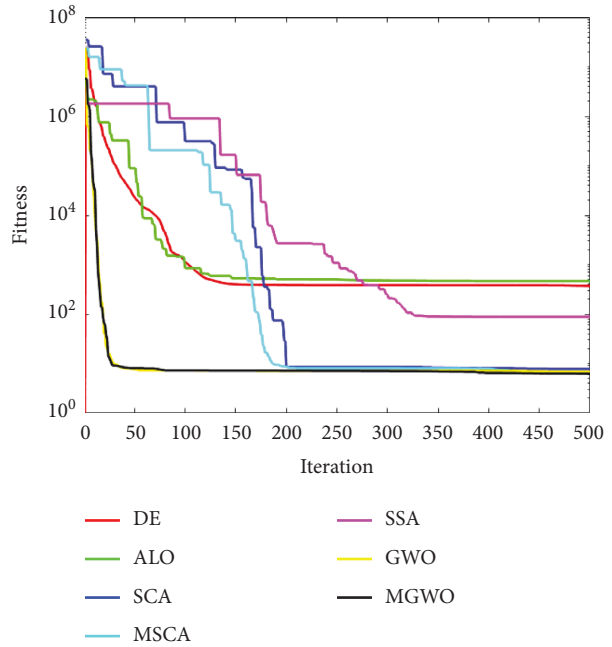


Figure 11: Convergence graph for $F5$ function.

(iii) The different responses such as interarea and local area oscillation responses, tie-line power response, and the response of injected voltage of SSSC are shown in Figures 37–41.

(iv) To demonstrate the effectiveness of MGWOA, fifteen independent simulations are run with MGWOA, GWO, SSA, MSCA, SCA, ALO, and DE.

(v) The average and standard deviations of fifteen independent simulations are given in Table 10. The table confirms that the proposed approach achieves the least mean value with respect to other techniques investigated.

(vi) Figure 42 depicts the convergence plot of various methods for the MMPS network, demonstrating

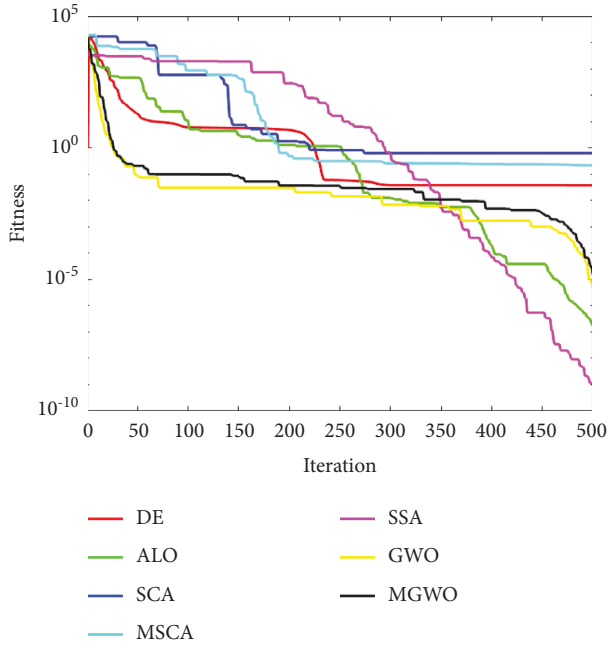


Figure 12: Convergence graph for *F6* function.

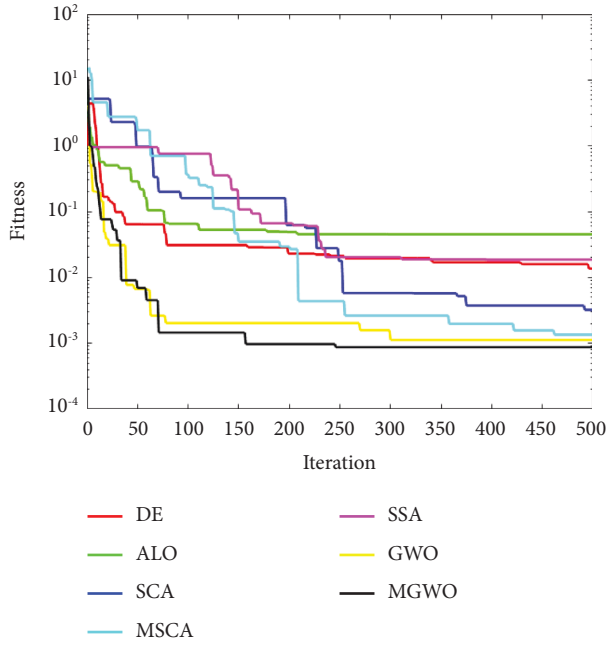


Figure 13: Convergence graph for *F7* function.

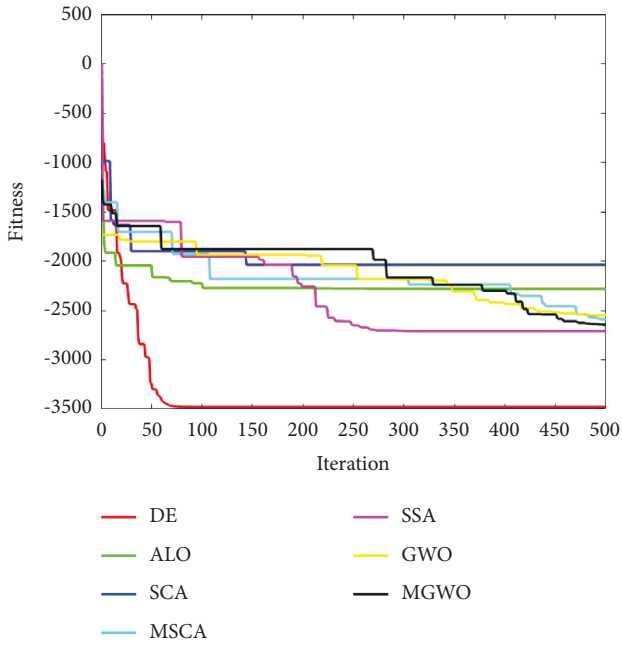


Figure 14: Convergence graph for *F*8 function.

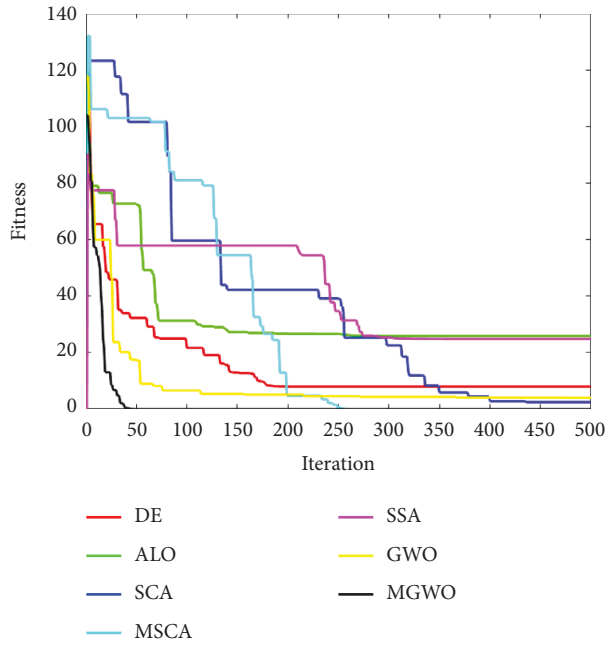


Figure 15: Convergence graph for *F*9 function.

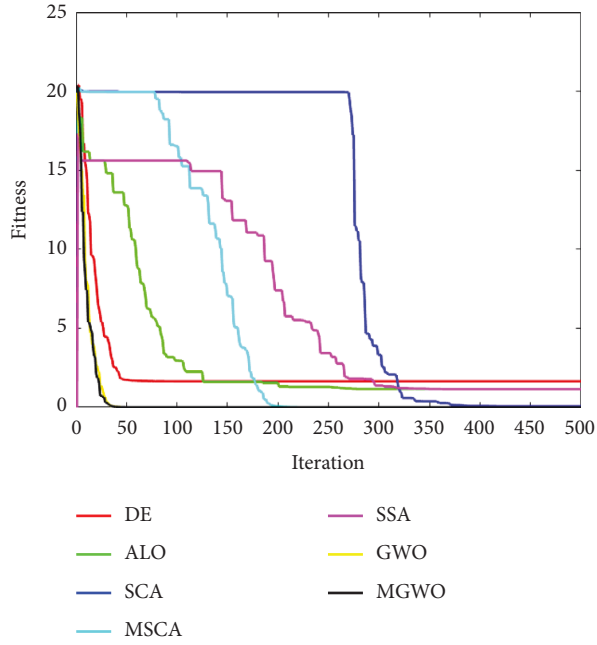


Figure 16: Convergence graph for $F10$ function.

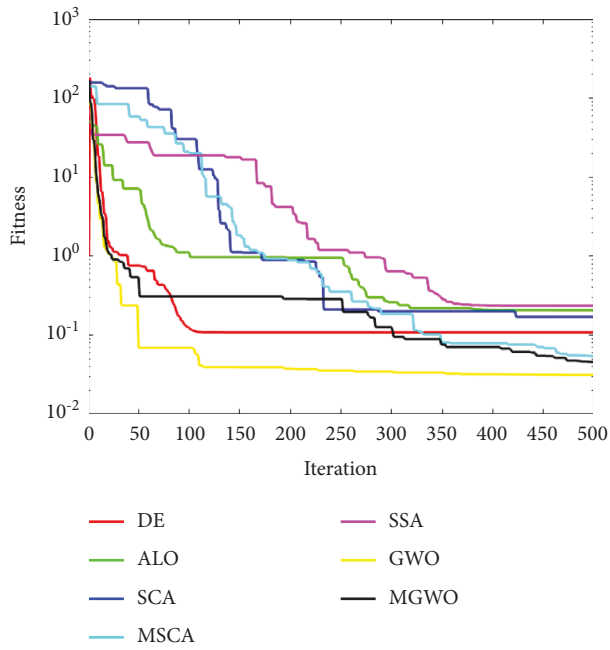


Figure 17: Convergence graph for $F11$ function.

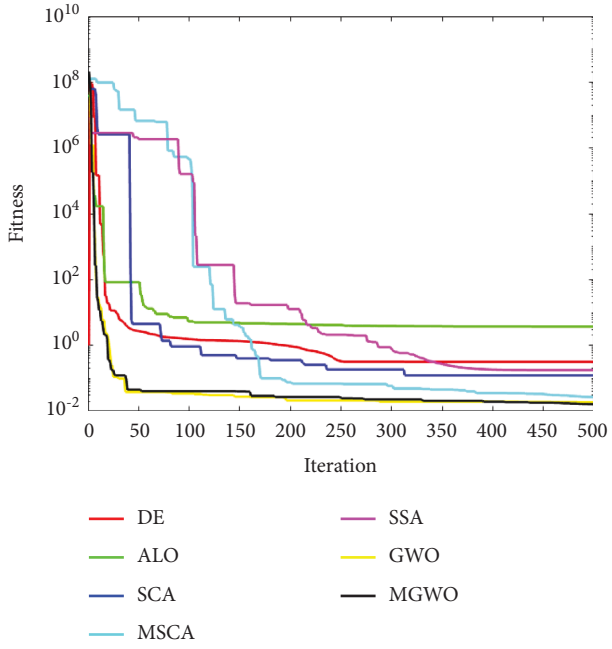


Figure 18: Convergence graph for $F12$ function.

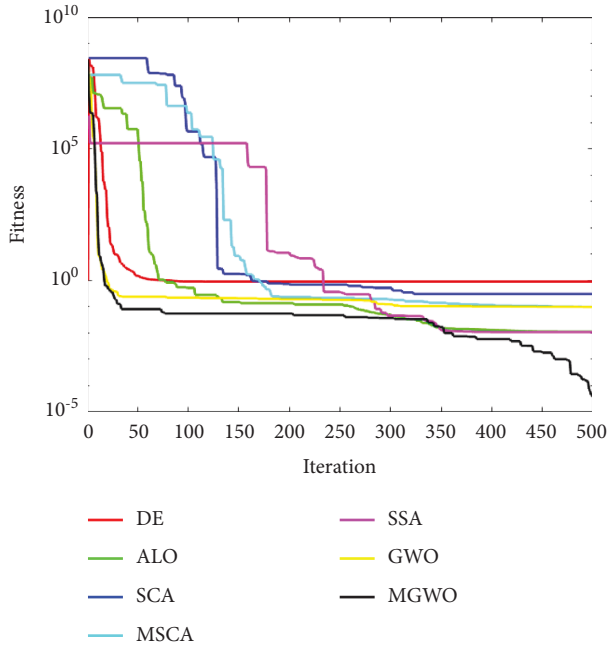


Figure 19: Convergence graph for $F13$ function.

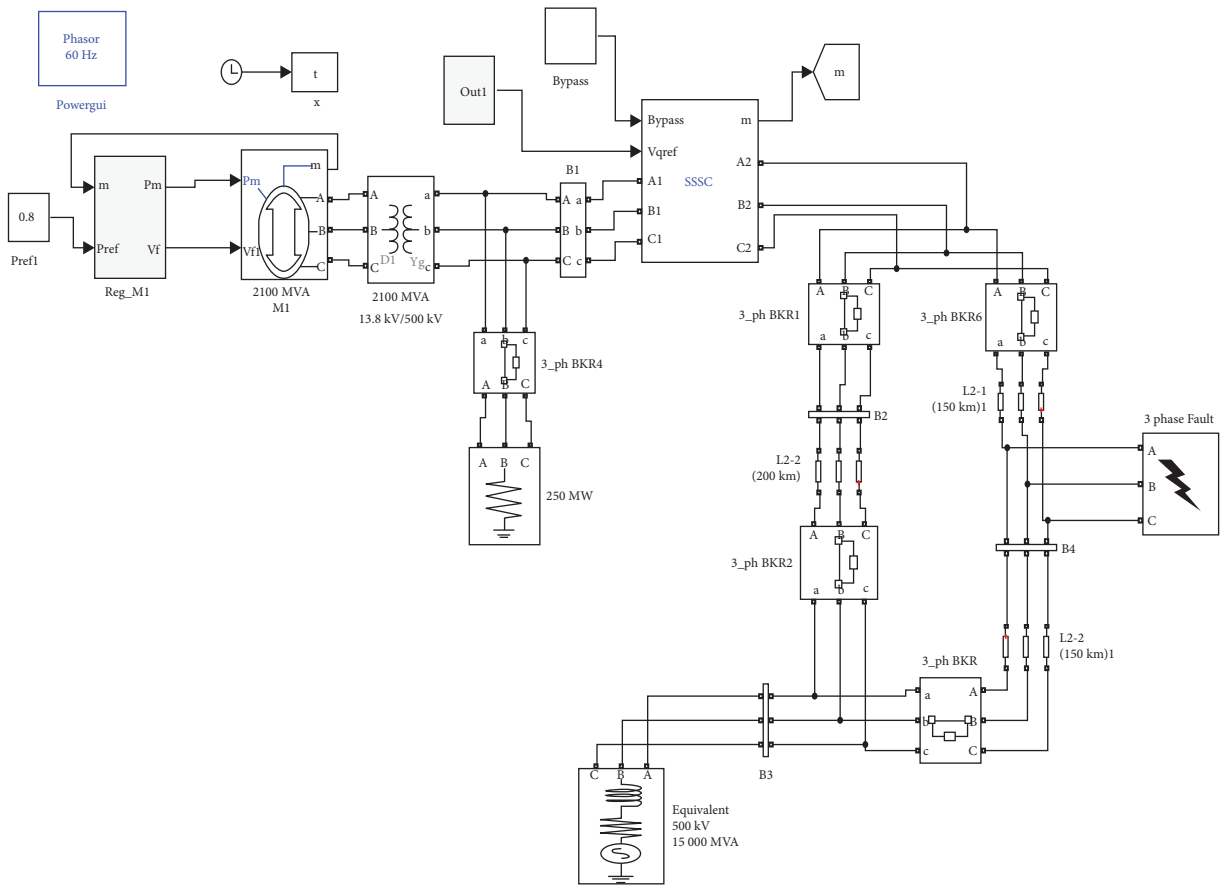


Figure 20: SIMULINK model of SMIB system.

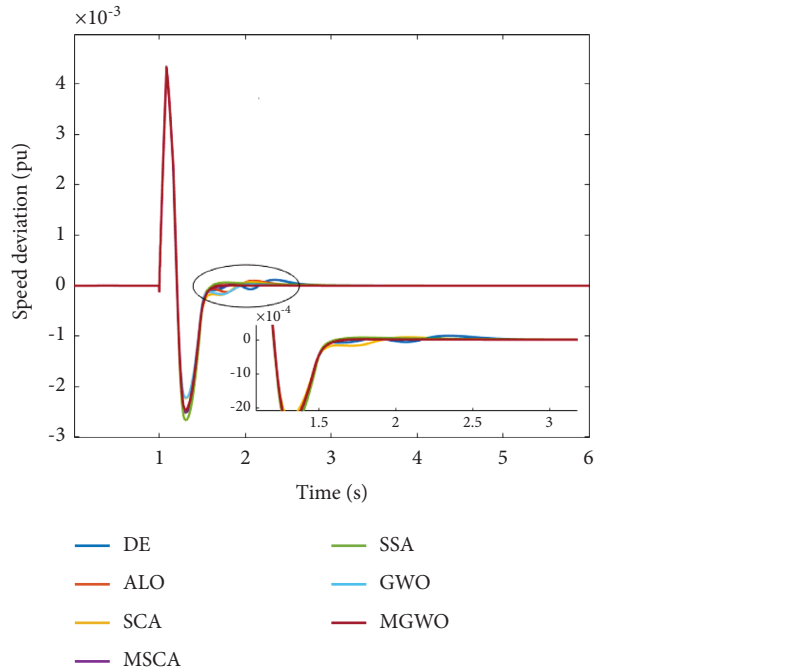


Figure 21: Speed deviation under NL.

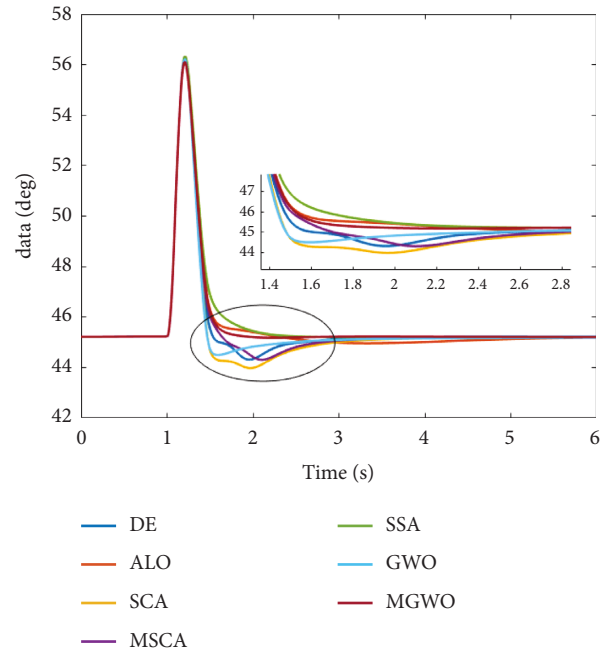


Figure 22: Power angle under NL.

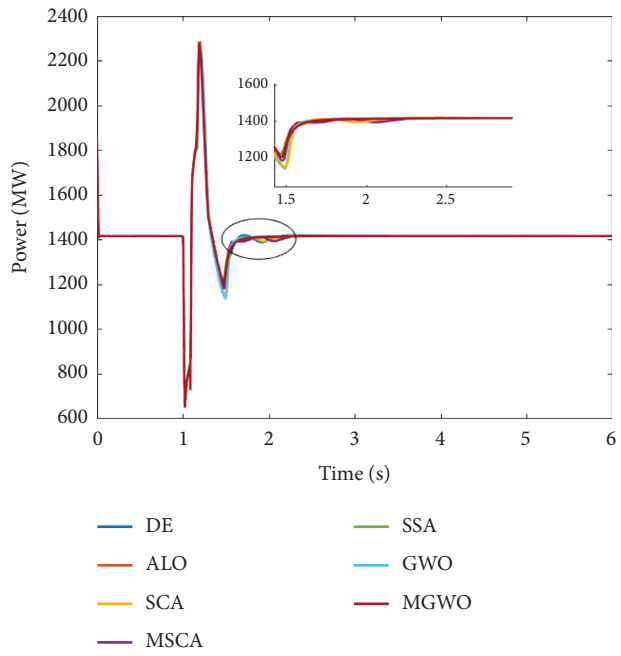


Figure 23: Tie-line power under NL.

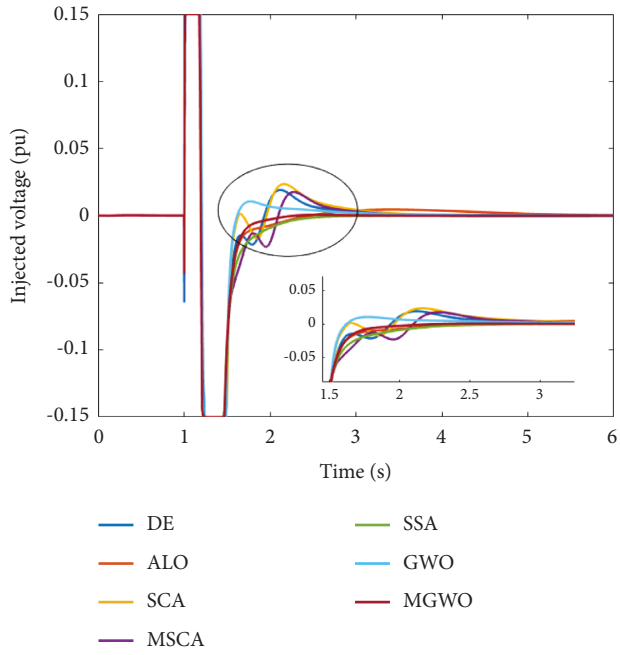


Figure 24: SSSC injected voltage under NL.

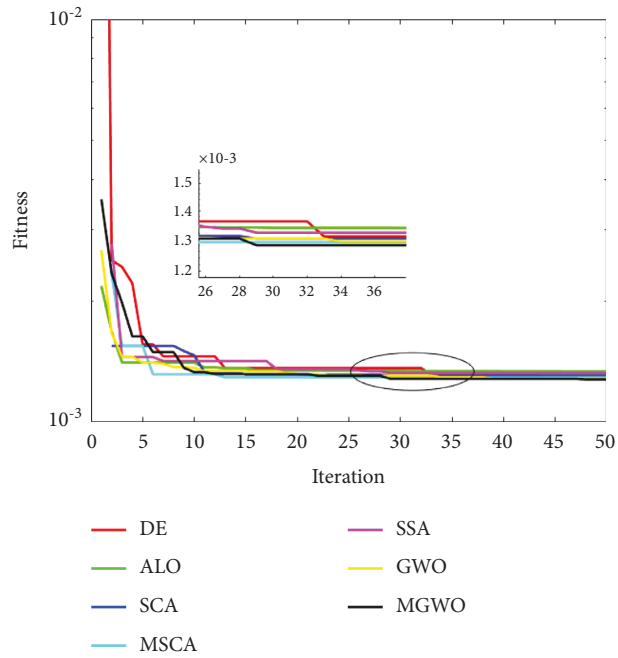


Figure 25: Convergence curve of different algorithms under NL condition.

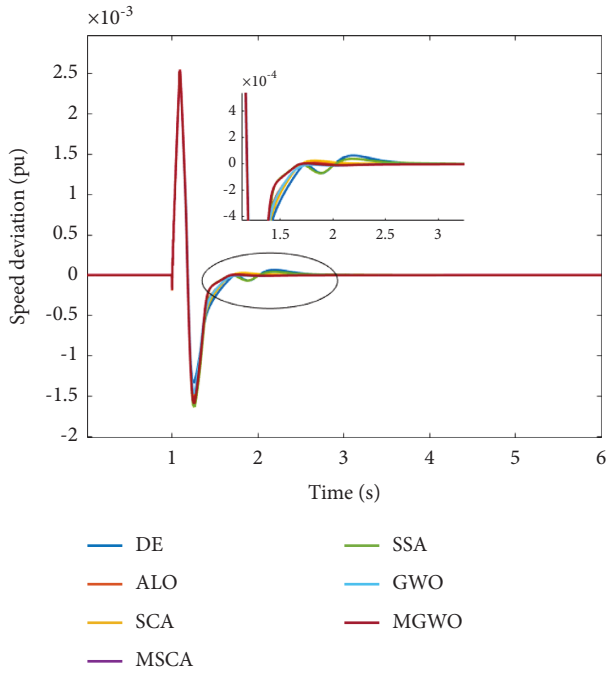


Figure 26: Plot for speed deviation under LL.

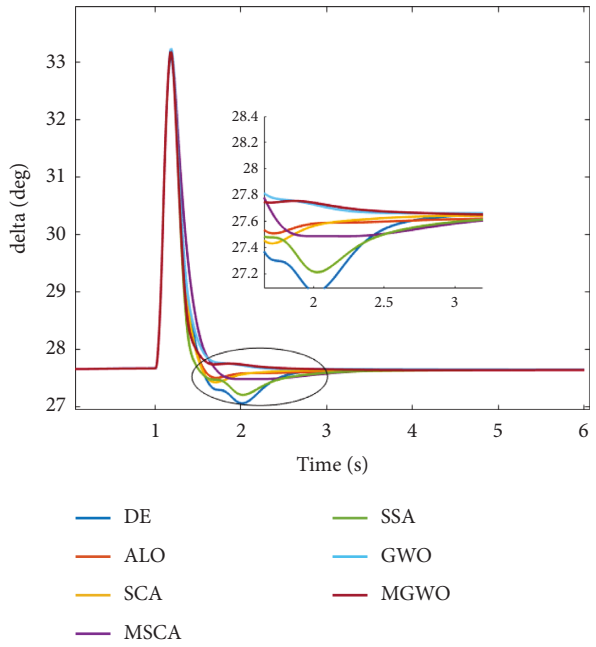


Figure 27: Plot for power angle under LL.

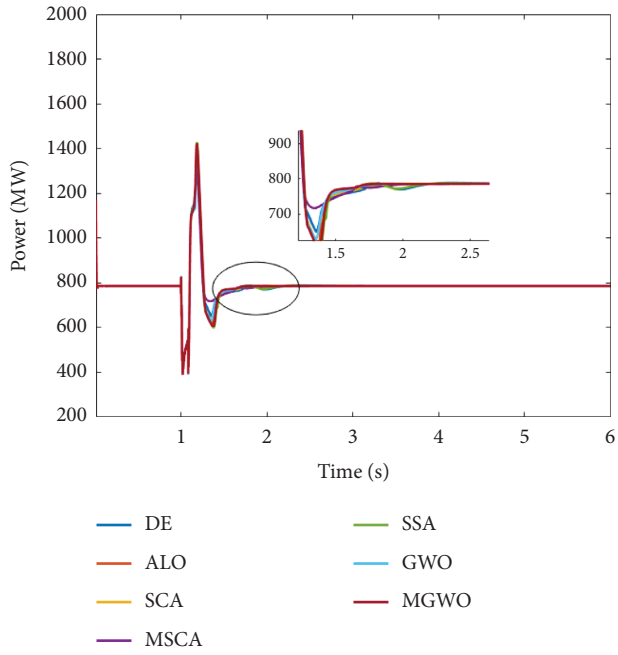


Figure 28: Plot for tie-line power under LL.

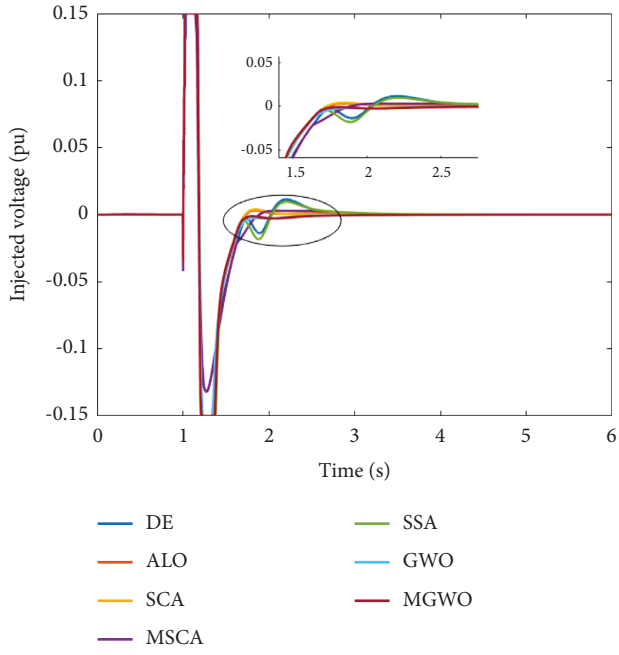


Figure 29: Plot for SSSC injected voltage under LL.

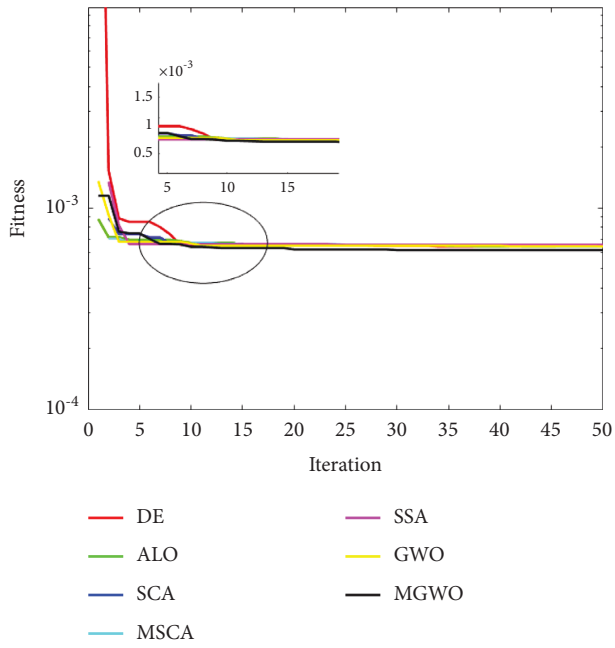


Figure 30: Convergence curve of different algorithms under LL conditions.

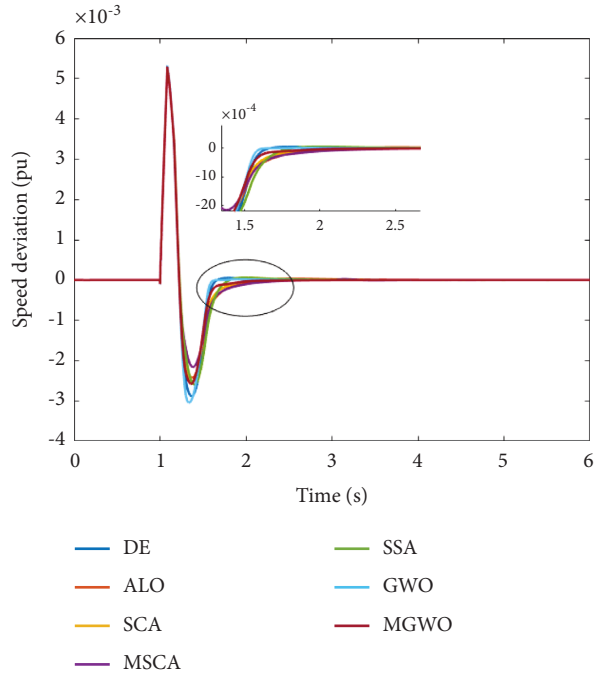


Figure 31: Speed deviation under HL.

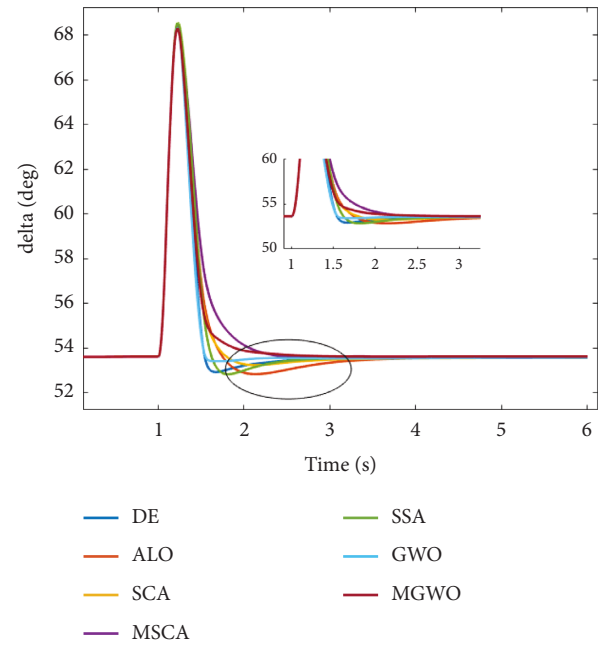


Figure 32: Power angle under HL.

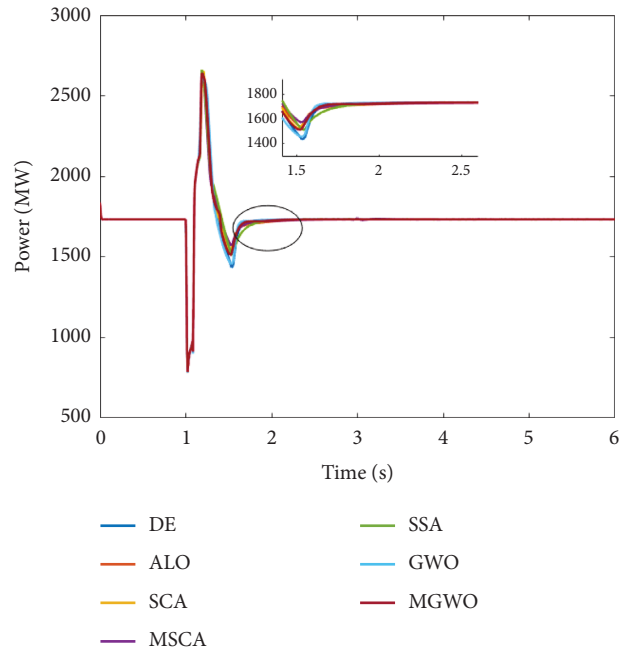


Figure 33: Tie-line power under HL.

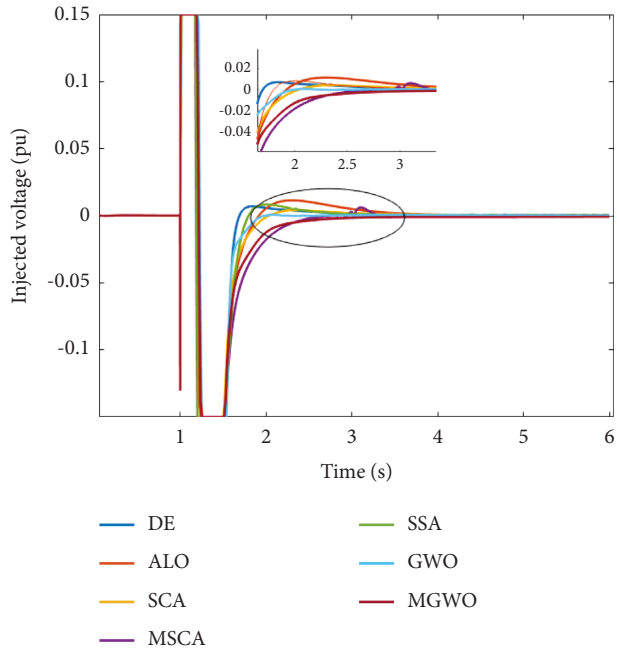


Figure 34: SSSC injected voltage under HL.

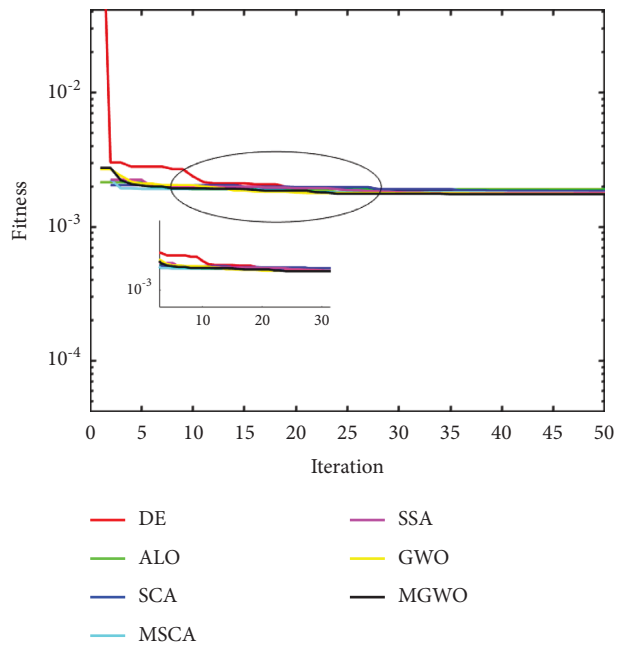


Figure 35: Convergence curve of different algorithms under HL conditions.

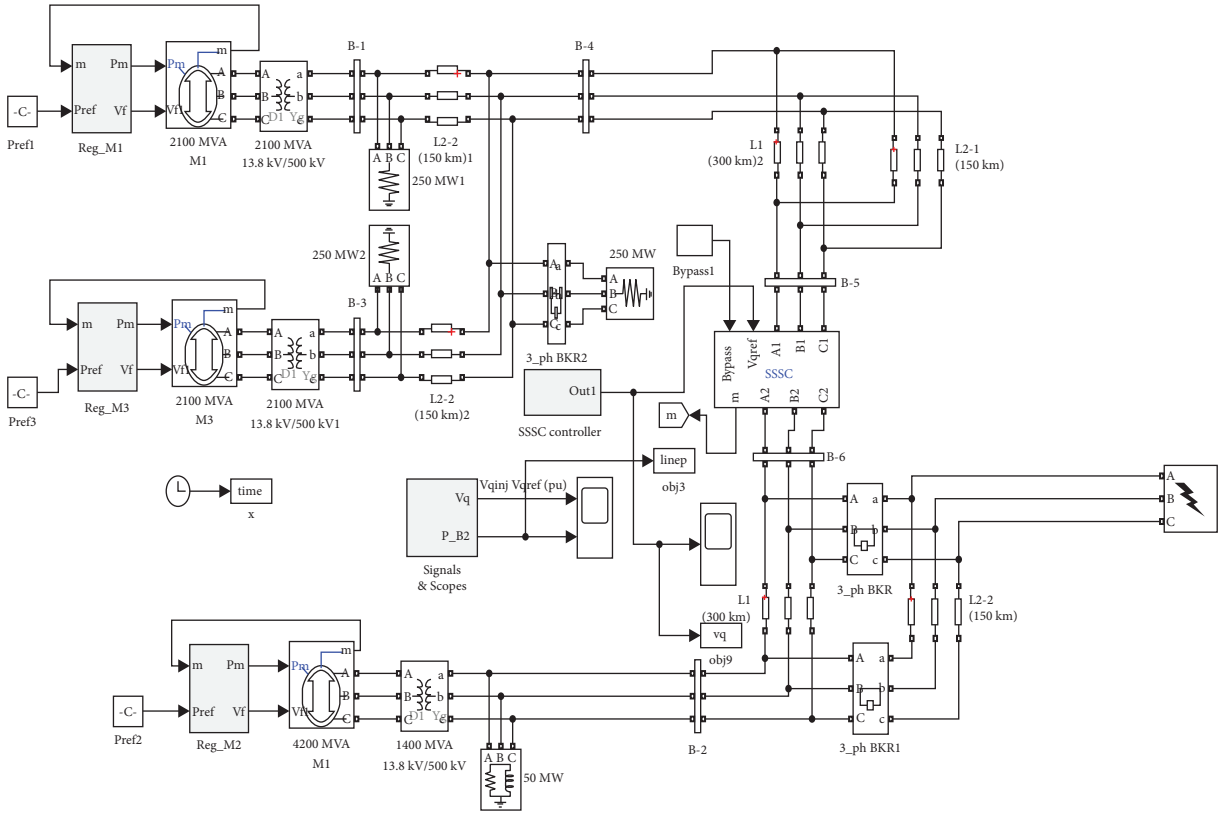


Figure 36: SIMULINK model for MMPS network.

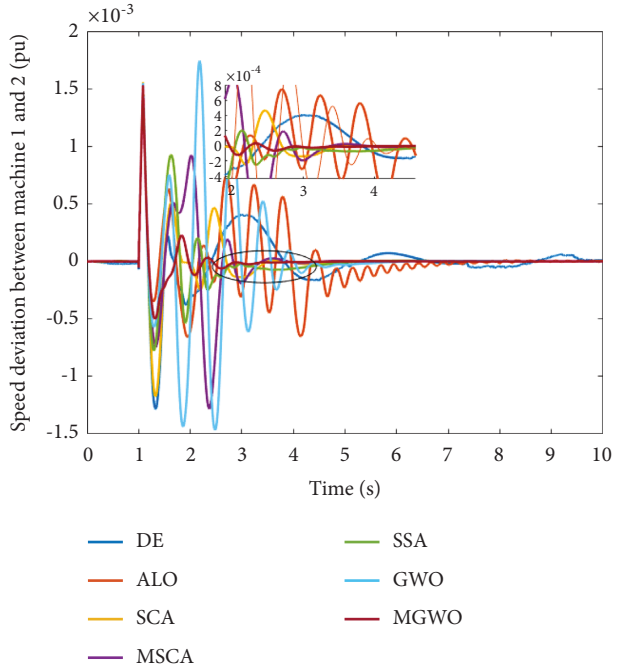


Figure 37: Interarea mode oscillations between machine 1 and 2.

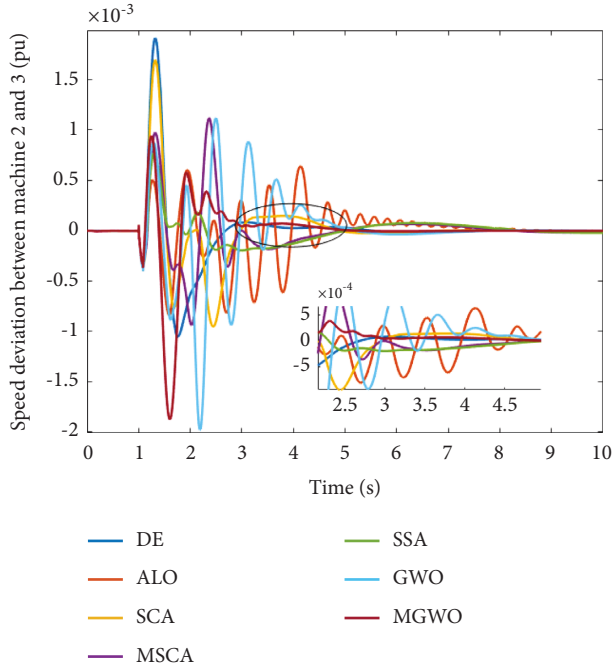


Figure 38: Interarea mode oscillations between machine 2 and 3.

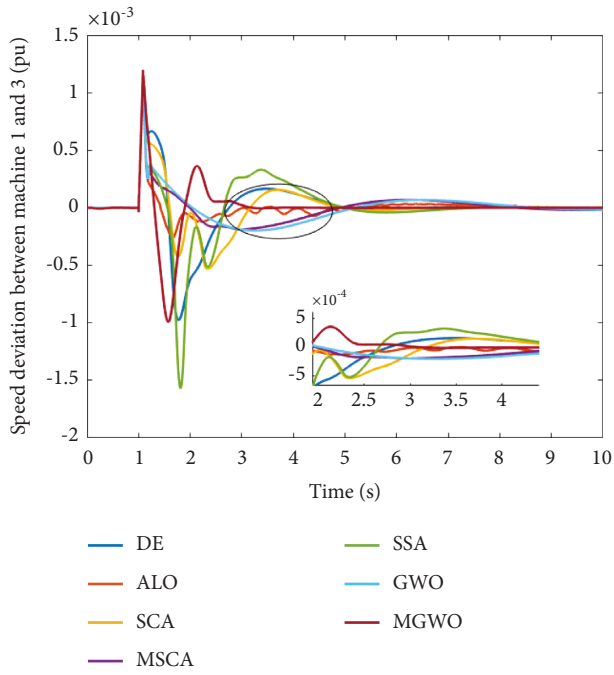


Figure 39: Local area mode oscillations between machine 1 and 3.

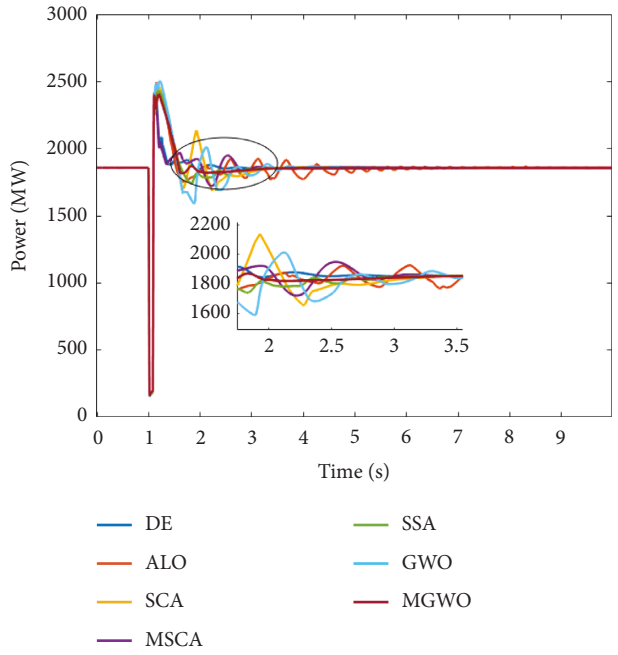


Figure 40: Tie-line power oscillation.

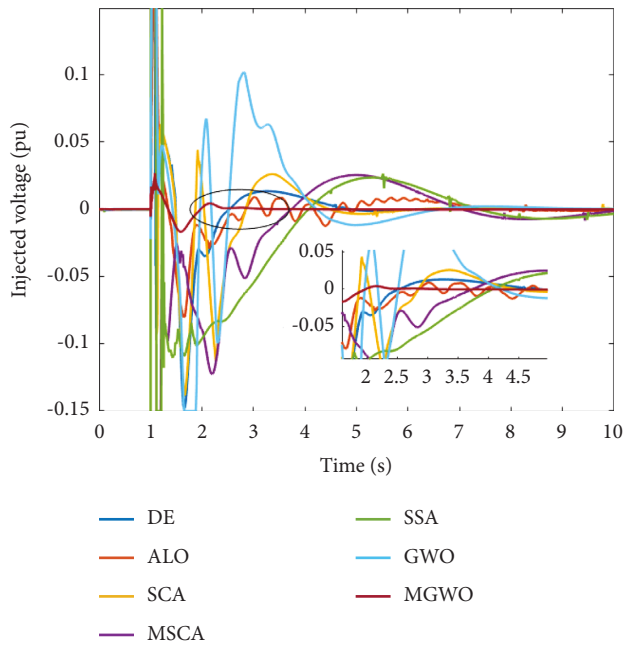


Figure 41: SSSC injected voltage.

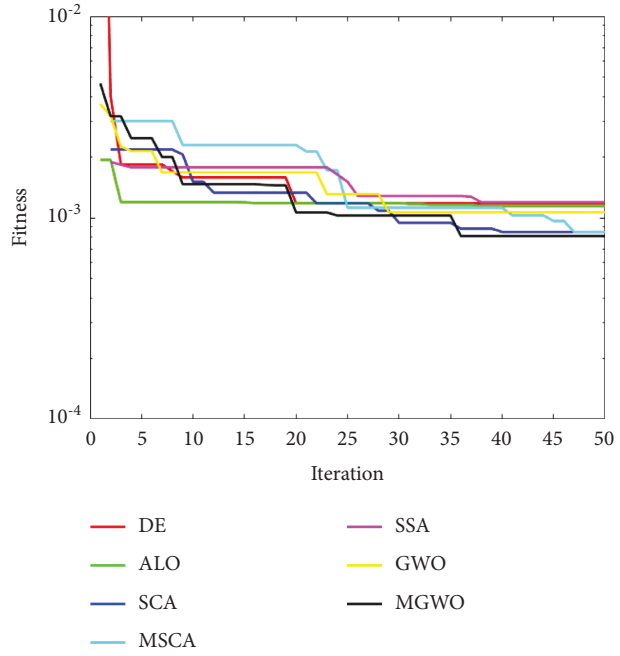


Figure 42: Convergence plot of different methods for MMPS.

Table 4: Comparison of fitness values of SMIB system under nominal loading using different algorithms (best values are presented in bold).

| | MGWO Mean ± Std. Dev | GWO Mean ± Std. Dev | SSA Mean ± Std. Dev | MSCA Mean ± Std. Dev | SCA Mean ± Std. Dev | ALO Mean ± Std. Dev | DE Mean ± Std. Dev |
|---|---|---|---|---|---|---|---|
| Fitness value | **0.001275 ± 9.1868 $E-$ 06** | 0.001288 ± $1E-05$ | 0.001313 ± $3.52E-05$ | 0.001291 ± $4.76E-06$ | 0.001307 ± $1.75E-05$ | 0.00133 ± $2.65E-05$ | 0.001289 ± $1.85E-05$ |

Table 5: Comparison of fitness values of SMIB system under light loading using different algorithms (best values are presented in bold).

| | MGWO Mean ± Std. Dev | GWO Mean ± Std. Dev | SSA Mean ± Std. Dev | MSCA Mean ± Std. Dev | SCA Mean ± Std. Dev | ALO Mean ± Std. Dev | DE Mean ± Std. Dev |
|---|---|---|---|---|---|---|---|
| Fitness value | **0.001275 ± 9.1868 $E-06$** | 0.001288 ± $1E-05$ | 0.001313 ± $3.52E-05$ | 0.001291 ± $4.76E-06$ | 0.001307 ± $1.75E-05$ | 0.00133 ± $2.65E-05$ | 0.001289 ± $1.85E-05$ |

Table 6: Comparison of fitness values of SMIB system under heavy loading using different algorithms (best values are presented in bold).

| | MGWO Mean ± Std. Dev | GWO Mean ± Std. Dev | SSA Mean ± Std. Dev | MSCA Mean ± Std. Dev | SCA Mean ± Std. Dev | ALO Mean ± Std. Dev | DE Mean ± Std. Dev |
|---|---|---|---|---|---|---|---|
| Fitness value | **0.001751 ± 1.47$E-05$** | 0.001769 ± $3.28E-05$ | 0.001814 ± $7.2E-05$ | 0.001824 ± $6.48E-05$ | 0.001841 ± $4.17E-05$ | 0.001896 ± $4.07E-05$ | 0.001802 ± $4.98E-05$ |

Table 7: Optimized PSS, FOPID, and SSSC controller parameters for SMIB system under nominal loading using different algorithms.

| Controller | Parameters | Methods | | | | | | |
|---|---|---|---|---|---|---|---|---|
| | | MGWO | GWO | SSA | MSCA | SCA | ALO | DE |
| PSS | $K_{PSS}$ | 8.9036 | 11.819 | 2.6522 | 0.1 | 72.873 | 1.5325 | 43.48 |
| | $T_{P1}$ | 0.18313 | 0.028318 | 0.019073 | 0.036231 | 0.01 | 0.98634 | 0.11085 |
| | $T_{P2}$ | 1.2977 | 1.5907 | 1.7938 | 0.62092 | 2 | 1.2069 | 1.8275 |
| | $T_{P3}$ | 0.12692 | 0.75905 | 1.1926 | 1.6886 | 0.086268 | 1.96 | 2 |
| | $T_{P4}$ | 0.67776 | 1.5441 | 1.6878 | 1.5351 | 2 | 0.57393 | 1.7251 |
| FOPID | $K_p$ | 96.81 | 96.853 | 95.699 | 74.146 | 100 | 86.34 | 65.934 |
| | $K_i$ | 74.217 | 87.58 | 16.984 | 45.259 | 100 | 2.9806 | 56.036 |
| | $\Lambda$ | 0.7456 | 0.17297 | 0.42971 | 0.01 | 0.013609 | 0.78447 | 0.74943 |
| | $K_d$ | 8.441 | 25.799 | 98.431 | 93.895 | 1.7932 | 56.429 | 100 |
| | $\mu$ | 0.0987 | 0.16799 | 0.01 | 0.01 | 0.01 | 0.22962 | 0.85238 |
| SSSC | $T_1$ | 0.7684 | 1.9725 | 0.020461 | 2 | 0.01 | 0.27533 | 1.5488 |
| | $T_2$ | 1.4483 | 1.5389 | 1.9628 | 2 | 0.01 | 0.79582 | 0.89567 |
| | $T_3$ | 2 | 1.9137 | 1.9558 | 0.01 | 0.01 | 1.7731 | 0.017744 |
| | $T_4$ | 0.67423 | 1.8947 | 0.01 | 0.010005 | 0.01 | 0.49587 | 0.85688 |

Table 8: Optimized PSS, FOPID, and SSSC controller parameters for SMIB system under light loading using different algorithms.

| Controller | Parameters | Methods | | | | | | |
|---|---|---|---|---|---|---|---|---|
| | | MGWO | GWO | SSA | MSCA | SCA | ALO | DE |
| PSS | $K_{PSS}$ | 6.4975 | 20.741 | 11.205 | 8.1731 | 0.1 | 13.244 | 32.128 |
| | $T_{P1}$ | 0.16116 | 0.15068 | 0.75378 | 0.61011 | 0.49758 | 0.25566 | 0.40465 |
| | $T_{P2}$ | 0.91014 | 0.98954 | 1.5766 | 0.16452 | 0.01 | 1.3846 | 0.90525 |
| | $T_{P3}$ | 0.44033 | 0.5467 | 0.42316 | 0.15504 | 0.020342 | 0.26681 | 0.33993 |
| | $T_{P4}$ | 1.1713 | 1.5697 | 0.97853 | 2 | 0.057318 | 1.5878 | 1.0891 |
| FOPID | $K_p$ | 22.336 | 86.373 | 99.999 | 89.81 | 86.463 | 90.203 | 53.812 |
| | $K_i$ | 99.967 | 100 | 25.397 | 87.907 | 100 | 58.986 | 53.932 |
| | $\lambda$ | 0.41706 | 0.31229 | 0.03905 | 0.75348 | 0.029216 | 0.71573 | 0.676 |
| | $K_d$ | 24.582 | 17.398 | 0.10102 | 14.798 | 0.1 | 0.1 | 83.621 |
| | $\mu$ | 0.24264 | 0.041254 | 1.5847 | 0.01 | 0.49837 | 0.062109 | 0.01 |
| SSSC | $T_1$ | 1.3348 | 0.61236 | 1.999 | 1.3665 | 2 | 1.4951 | 1.0977 |
| | $T_2$ | 1.1364 | 0.6498 | 1.6114 | 0.82905 | 2 | 0.82886 | 1.7915 |
| | $T_3$ | 0.61354 | 0.55581 | 1.9408 | 1.6279 | 0.01 | 2 | 1.9368 |
| | $T_4$ | 0.46031 | 0.43714 | 1.6327 | 1.2522 | 0.01 | 1.655 | 0.93635 |

Table 9: Optimized PSS, FOPID, and SSSC controller parameters for SMIB system under heavy loading using different algorithms.

| Controller | Parameters | Methods | | | | | | |
|---|---|---|---|---|---|---|---|---|
| | | MGWO | GWO | SSA | MSCA | SCA | ALO | DE |
| PSS | $K_{PSS}$ | 0.41222 | 0.17214 | 3.342 | 3.1844 | 4.8211 | 2.7009 | 11.931 |
| | $T_{P1}$ | 1.7791 | 1.9734 | 0.03391 | 0.92493 | 0.25756 | 1.3142 | 0.097057 |
| | $T_{P2}$ | 1.0235 | 0.13714 | 1.621 | 1.072 | 0.010057 | 1.8423 | 1.5947 |
| | $T_{P3}$ | 1.667 | 0.49494 | 0.35423 | 1.9457 | 0.062757 | 0.16929 | 1.2685 |
| | $T_{P4}$ | 0.12634 | 0.18735 | 0.52289 | 1.2695 | 0.2197 | 0.055331 | 1.6826 |
| FOPID | $K_p$ | 85.43 | 53.305 | 99.218 | 100 | 95.845 | 61.352 | 75.248 |
| | $K_i$ | 100 | 77.242 | 0.1428 | 0.1046 | 0.11487 | 17.477 | 38.136 |
| | $\lambda$ | 0.67326 | 0.59578 | 1.8004 | 0.66122 | 0.063032 | 0.44118 | 0.73665 |
| | $K_d$ | 1.333 | 44.808 | 99.376 | 100 | 0.12645 | 12.161 | 20.192 |
| | $\mu$ | 1.0765 | 0.013508 | 0.010594 | 0.010109 | 0.042036 | 0.35343 | 0.01 |
| SSSC | $T_1$ | 1.1306 | 0.95576 | 0.27675 | 0.028811 | 1.7464 | 1.5801 | 1.8365 |
| | $T_2$ | 0.64344 | 1.2547 | 0.01509 | 0.012875 | 0.011116 | 1.5895 | 1.1827 |
| | $T_3$ | 1.8471 | 1.9288 | 0.053658 | 0.026783 | 0.011112 | 1.639 | 1.6554 |
| | $T_4$ | 1.8468 | 0.77681 | 0.30398 | 0.010033 | 1.3872 | 0.91417 | 1.5016 |

Table 10: Comparison of fitness values of MMPS using different algorithms.

| | MGWO Mean ± Std. Dev | GWO Mean ± Std. Dev | SSA Mean ± Std. Dev | MSCA Mean ± Std. Dev | SCA Mean ± Std. Dev | ALO Mean ± Std. Dev | DE Mean ± Std. Dev |
|---|---|---|---|---|---|---|---|
| Fitness value | **0.000828 ± 0.000180323** | 0.001019 ± 0.000236 | 0.001313 ± 0.000387 | 0.000896 ± 0.000325 | 0.001273 ± 0.000249 | 0.001096 ± 0.000262 | 0.001134 ± 0.000351 |

Table 11: Optimized FOPID, SSSC, and PSS controller parameters for MMPS using different algorithms.

| Controller | Parameters | Methods | | | | | | |
|---|---|---|---|---|---|---|---|---|
| | | MGWO | GWO | SSA | MSCA | SCA | ALO | DE |
| FOPID | $K_p$ | 0.1 | 41.545 | 61.311 | 74.392 | 0.14318 | 50.286 | 65.072 |
| | $K_i$ | 71.77 | 41.226 | 20.636 | 53.291 | 99.723 | 0.17322 | 31.123 |
| | $\lambda$ | 0.97684 | 1.083 | 1.833 | 0.32829 | 0.040326 | 0.81888 | 0.22795 |
| | $K_d$ | 92.822 | 53.564 | 0.6006 | 7.1243 | 0.11122 | 50.422 | 29.487 |
| | $\mu$ | 0.02514 | 0.30118 | 1.139 | 0.013796 | 0.015131 | 0.011316 | 0.82455 |
| SSSC | $T_1$ | 1.9564 | 1.6751 | 0.47875 | 0.37173 | 0.46135 | 1.9325 | 1.4246 |
| | $T_2$ | 0.04086 | 1.6478 | 1.6287 | 0.027048 | 0.01 | 0.7054 | 1.3761 |
| | $T_3$ | 1.2467 | 1.5923 | 0.4412 | 1.9081 | 0.067586 | 1.2637 | 1.3824 |
| | $T_4$ | 0.69539 | 0.65322 | 0.4706 | 0.38856 | 0.1457 | 1.312 | 1.9275 |
| PSS-1 | $K_{PSS1}$ | 35.93 | 31.055 | 57.215 | 7.5808 | 0.45023 | 58.589 | 63.357 |
| | $T_{11}$ | 1.1492 | 0.4976 | 0.14494 | 0.016107 | 0.014845 | 0.85848 | 1.9815 |
| | $T_{12}$ | 1.362 | 1.4957 | 1.1524 | 0.10655 | 0.049633 | 1.1891 | 0.01 |
| | $T_{13}$ | 0.71416 | 0.33091 | 0.045735 | 0.014321 | 0.57545 | 0.56574 | 2 |
| | $T_{14}$ | 0.011857 | 1.3188 | 0.013399 | 1.8492 | 0.28281 | 0.01135 | 1.7955 |
| PSS-2 | $K_{PSS2}$ | 47.299 | 50.243 | 70.374 | 40.214 | 41.879 | 59.389 | 24.245 |
| | $T_{21}$ | 1.5947 | 0.45002 | 0.60677 | 0.19067 | 0.50821 | 0.52835 | 0.85604 |
| | $T_{22}$ | 0.0149 | 0.15123 | 1.1896 | 0.1453 | 0.44008 | 0.98824 | 0.85422 |
| | $T_{23}$ | 0.46636 | 0.069609 | 1.0891 | 1.1026 | 0.019905 | 0.58475 | 0.95996 |
| | $T_{24}$ | 0.50423 | 0.58404 | 1.9422 | 0.013974 | 0.015181 | 0.85638 | 0.52148 |
| PSS-3 | $K_{PSS3}$ | 34.703 | 49.156 | 88.088 | 31.043 | 9.6339 | 97.934 | 76.065 |
| | $T_{31}$ | 1.9933 | 1.3316 | 1.5388 | 0.18964 | 0.077045 | 1.7234 | 0.6584 |
| | $T_{32}$ | 1.7779 | 1.3705 | 1.5652 | 1.8885 | 0.21533 | 0.92712 | 1.5844 |
| | $T_{33}$ | 1.9597 | 1.0882 | 0.70425 | 1.8317 | 1.6221 | 1.4251 | 1.2079 |
| | $T_{34}$ | 1.9857 | 0.67919 | 0.13721 | 0.034354 | 0.01 | 0.61906 | 0.01 |

the superiority of the proposed MGWOA approach over other methods.

(vii) Table 11 shows the optimum parameters of PSS, FOPID, and SSSC controllers for the MMPS network achieved using the proposed MGWOA approach.

## 8. Conclusion

In this study, the design of FOPID-based damping controllers is presented for enhancing power system stability. A time-domain simulation-based objective function to minimize power system oscillations is used to solve the proposed controllers design challenge. Testing the proposed MGWOA approach on 13 benchmark functions reveals that it achieves faster convergence than its counterparts. The MGWOA technique is then used to tune the controller parameters in an optimal and coordinated manner. The efficacy of the suggested coordinated design approach is demonstrated using simulation results under various loading conditions and disturbances. Furthermore, the coordinated design of PSS and SSSC is applied to a multimachine power system network, and simulation results are shown to demonstrate the proposed controllers' effectiveness in damping oscillations in a multimachine power system. The statistical analysis has been performed to validate the robustness of the proposed method with respect to other methods. The simulation findings indicate that the proposed MGWOA technique can be used to increase the stability of a real-world power system.

## Appendix

### a. SMIB system

Generator: 2100 MVA, VB = 13.8 kV, and $f$ = 60 Hz

Transformer: 13.8/500 kV, 60 Hz, and 2100 MVA

Transmission line: length = 300 km, 3-phase, and 60 Hz

Power system stabilizer: washout time constant $T_W$ = 10 s and limit of $V_s$ = ± 0.15

### b. MMPS

Generators: SB1 = SB3 = 2100 MVA, SB2 = 4200 MVA, VB = 13.8 kV, and $f$ = 60 Hz

Loads: load 1 = load 3 = 250 MW and load 2 = 50 MW

Transformers: 13.8/500 kV, $f = 60$ Hz, SBT1 = SBT3 = 2100 MVA, and SBT2 = 1400 MVA

Injected voltage magnitude limit: $V_q = \pm 0.2$

Machine 1: $P_{e1} = 1280$ MW (0.6095 pu)

Machine 2: $P_{e2} = 3480.6$ MW (0.8287 pu)

Machine 3: $P_{e3} = 880$ MW (0.419 pu)

## Data Availability

The data used to support the findings of the study can be obtained from the corresponding author upon request.

## Conflicts of Interest

The authors declare that they have no conflicts of interest.

## References


[1] P. Kundur, *Power System Stability and Control*, Mc-Grall Hill, New York, NY, USA, 1994.

[2] K. Bhattacharya, J. Nanda, and M. L. Kothari, "Optimization and performance analysis of conventional power system stabilizers," *International Journal of Electrical Power & Energy Systems*, vol. 19, no. 7, pp. 449–458, 1997.

[3] T. Hussein, M. S. Saad, A. L. Elshafei, and A. Bahgat, "Damping inter-area modes of oscillation using an adaptive fuzzy power system stabilizer," *Electric Power Systems Research*, vol. 80, no. 12, pp. 1428–1436, 2010.

[4] E. S. Ali, "Optimization of power system stabilizers using BAT search algorithm," *International Journal of Electrical Power & Energy Systems*, vol. 61, pp. 683–690, 2014.

[5] P. Zhang and A. H. Coonick, "Coordinated synthesis of PSS parameters in multi-machine power systems using the method of inequalities applied to genetic algorithms," *IEEE Transactions on Power Systems*, vol. 15, no. 2, pp. 811–816, 2000.

[6] M. Jebali, O. Kahouli, and H. Hadj Abdallah, "Optimizing PSS parameters for a multi-machine power system using genetic algorithm and neural network techniques," *International Journal of Advanced Manufacturing Technology*, vol. 90, pp. 2669–2688, 2017.

[7] N. G. Hingoran and L. Gyugyi, *Understanding FACTS Concepts and Technology of Flexible AC Transmission Systems*, Wiley-IEEE Press, New Jersey, NJ, USA, 2000.

[8] L. Gyugyi, C. D. Schauder, and K. K. Sen, "Static synchronous series compensator: a solid-state approach to the series compensation of transmission lines," *IEEE Transactions on Power Delivery*, vol. 12, no. 1, pp. 406–417, 1997.

[9] H. F. Wang, "Static synchronous series compensator to damp power system oscillations," *Electric Power Systems Research*, vol. 54, no. 2, pp. 113–119, 2000.

[10] A. L. B. Do Bomfim, G. N. Taranto, and D. M. Falcao, "Simultaneous tuning of power system damping controllers using genetic algorithms," *IEEE Transactions on Power Systems*, vol. 15, no. 1, pp. 163–169, 2000.

[11] L. J. Cai and I. Erlich, "Simultaneous coordinated tuning of PSS and FACTS damping controllers in large power systems," *IEEE Transactions on Power Systems*, vol. 20, no. 1, pp. 294–300, 2005.

[12] S. Panda, S. C. Swain, P. K. Rautray, R. K. Malik, and G. Panda, "Design and analysis of SSSC-based supplementary damping controller," *Simulation Modelling Practice and Theory*, vol. 18, no. 9, pp. 1199–1213, 2010.

[13] S. Panda, "Differential evolution algorithm for SSSC-based damping controller design considering time delay," *Journal of the Franklin Institute*, vol. 348, no. 8, pp. 1903–1926, 2011.

[14] S. Panda, "Multi-objective evolutionary algorithm for SSSC-based controller design," *Electric Power Systems Research*, vol. 79, no. 6, pp. 937–944, 2009.

[15] S. Panda, "Robust coordinated design of multiple and multi-type damping controller using differential evolution algorithm," *International Journal of Electrical Power & Energy Systems*, vol. 33, no. 4, pp. 1018–1030, 2011.

[16] M. S. Widyan, "Controlling chaos and bifurcations of SMIB power system experiencing SSR phenomenon using SSSC," *International Journal of Electrical Power & Energy Systems*, vol. 49, pp. 66–75, 2013.

[17] T. R. Jyothsna and K. Vaisakh, "Effects of strong resonance in multi-machine power systems with SSSC supplementary modulation controller," *International Transactions on Electrical Energy Systems*, vol. 23, no. 1, pp. 24–47, 2013.

[18] E. Gholipour and S. M. Nosratabadi, "A new coordination strategy of SSSC and PSS controllers in power system using SOA algorithm based on Pareto method," *International Journal of Electrical Power & Energy Systems*, vol. 67, pp. 462–471, 2015.

[19] D. Butti, S. K. Mangipudi, and S. R. Rayapudi, "An improved whale optimization algorithm for the design of multi-machine power system stabilizer," *International Transactions on Electrical Energy Systems*, vol. 30, no. 5, Article ID e12314, 202.

[20] M. K. Kar, S. Kumar, A. K. Singh, and S. Panigrahi, "A modified sine cosine algorithm with ensemble search agent updating schemes for small signal stability analysis," *International Transactions on Electrical Energy Systems*, vol. 31, no. 11, Article ID e13058, 2021.

[21] D. Murali, M. Rajaram, and N. Reka, "Comparison of FACTS devices for power system stability enhancement," *International Journal of Computer Application*, vol. 8, no. 4, pp. 30–35, 2010.

[22] A. Ghasemi-Marzbali and R. Ahmadiahangar, "A coordinated strategy for multi-machine power system stability," *Applied Soft Computing*, vol. 110, Article ID 107742, 2021.

[23] D. Butti, S. K. Mangipudi, and S. Rayapudi, "Model order reduction based power system stabilizer design using improved whale optimization algorithm," *IETE Journal of Research*, pp. 1–20, 2021.

[24] A. Yakout, W. Sabry, and H. M. Hasanien, "Enhancing rotor angle stability of power systems using marine predator algorithm based cascaded PID control," *Ain Shams Engineering Journal*, vol. 12, no. 2, pp. 1849–1857, 2021.

[25] I. Podlubny, "Fractional-order systems and PI/sup/spl lambda//D/sup/spl mu//-controllers/spl lambda//D/sup/spl mu//-controllers," *IEEE Transactions on Automatic Control*, vol. 44, no. 1, pp. 208–214, 1999.

[26] A. Biswas, S. Das, A. Abraham, and S. Dasgupta, "Design of fractional-order PI$\lambda$D$\mu$ controllers with an improved differential evolution," *Engineering Applications of Artificial Intelligence*, vol. 22, no. 2, pp. 343–350, 2009.

[27] Y. Luo, Y. Q. Chen, C. Y. Wang, and Y. G. Pi, "Tuning fractional order proportional integral controllers for fractional order systems," *Journal of Process Control*, vol. 20, no. 7, pp. 823–831, 2010.

[28] L. Chaib, A. Choucha, and S. Arif, "Optimal design and tuning of novel fractional order PID power system stabilizer using a

new metaheuristic Bat algorithm," *Ain Shams Engineering Journal*, vol. 8, no. 2, pp. 113–125, 2017.

[29] M. S. Ayas and E. Sahin, "FOPID controller with fractional filter for an automatic voltage regulator," *Computers & Electrical Engineering*, vol. 90, Article ID 106895, 2021.

[30] P. R. Sahu, P. K. Hota, and S. Panda, "Modified whale optimization algorithm for fractional-order multi-input SSSC-based controller design," *Optimal Control Applications and Methods*, vol. 39, no. 5, pp. 1802–1817, 2018.

[31] S. Gurung, F. Jurado, S. Naetiladdanon, and A. Sangswang, "Comparative analysis of probabilistic and deterministic approach to tune the power system stabilizers using the directional bat algorithm to improve system small-signal stability," *Electric Power Systems Research*, vol. 181, Article ID 106176, 2020.

[32] D. Izci, "A novel improved atom search optimization algorithm for designing power system stabilizer," *Evolutionary Intelligence*, vol. 15, no. 3, pp. 2089–2103, 2021.

[33] W. Du, W. Dong, Y. Wang, and H. Wang, "A method to design power system stabilizers in a multi-machine power system based on single-machine infinite-bus system model," *IEEE Transactions on Power Systems*, vol. 36, no. 4, pp. 3475–3486, 2021.

[34] H. Verdejo, V. Pino, W. Kliemann, C. Becker, and J. Delpiano, "Implementation of particle swarm optimization (PSO) algorithm for tuning of power system stabilizers in multimachine electric power systems," *Energies*, vol. 13, no. 8, p. 2093, 2020.

[35] R. Devarapalli, B. Bhattacharyya, N. K. Sinha, and B. Dey, "Amended GWO approach based multi-machine power system stability enhancement," *ISA Transactions*, vol. 109, pp. 152–174, 2021.

[36] R. Devarapalli and B. Bhattacharyya, "A hybrid modified grey wolf optimization-sine cosine algorithm-based power system stabilizer parameter tuning in a multimachine power system," *Optimal Control Applications and Methods*, vol. 41, no. 4, pp. 1143–1159, 2020.

[37] P. R. Sahu, P. K. Hota, S. Panda, H. V. Long, and T. Allahviranloo, "Modified grasshopper optimization algorithm optimized adaptive fuzzy lead-lag controller for coordinated design of FACTS controller with PSS," *Journal of Intelligent and Fuzzy Systems*, vol. 43, pp. 1–20, 2022.

[38] N. Nahak, O. Satapathy, and P. Sengupta, "A new optimal static synchronous series compensator-governor control action for small signal stability enhancement of random renewable penetrated hydro-dominated power system," *Optimal Control Applications and Methods*, vol. 43, no. 3, pp. 593–617, 2022.

[39] N. Nahak and R. K. Mallick, "Investigation and damping of low-frequency oscillations of stochastic solar penetrated power system by optimal dual UPFC," *IET Renewable Power Generation*, vol. 13, no. 3, pp. 376–388, 2019.

[40] S. Mirjalili, S. M. Mirjalili, and A. Lewis, "Grey wolf optimizer," *Advances in Engineering Software*, vol. 69, pp. 46–61, 2014.

[41] M. K. Kar, S. Kumar, A. K. Singh, and S. Panigrahi, "Reactive power management by using a modified differential evolution algorithm," *Optimal Control Applications and Methods*, 2021.

[42] L. Kumar, M. K. Kar, and S. Kumar, "Statistical analysis based reactive power optimization using improved differential evolutionary algorithm," *Expert Systems*, Article ID e13091, 2022.